WRITHE-LIKE INVARIANTS OF ALTERNATING LINKS

by

Van Anh Pham

A dissertation submitted to the faculty of
The University of North Carolina at Charlotte
in partial fulfillment of the requirements
for the degree of Doctor of Philosophy in
Applied Mathematics

Charlotte

2022

Approved by:

_____
Dr. Yuanan Diao

_____
Dr. Gabor Hetyei

_____
Dr. Alan Dow

_____
Dr. Jose Gamez

ABSTRACT

VAN ANH PHAM. Writhe-like invariants of alternating links. (Under the direction of DR. YUANAN DIAO)

This dissertation introduces new invariants for a large class of links in knot theory, called alternating links. It also analyzes the strength of these invariants, that we call writhe-like invariants, in comparison with other general link invariants, and explores how these quantities can be used in solving other knot theory problems. A part of the dissertation is dedicated to describing the computer program that computes a few writhe-like invariants of alternating knots of n crossings, and reports on the computed data of alternating knots up to 12 crossings.

DEDICATION

This dissertation is dedicated to my first teacher of knot theory, Dr. Claus Ernst; and to my family, who have given me unconditional love and support throughout my higher education pursuit.

ACKNOWLEDGEMENTS

I would like to express my foremost gratitude to my advisor, professor Yuanan Diao, for his immense motivation, patience, and support of my study. Professor Diao is not only a mathematician that I look up to, but also my mentor inside and outside of my academic life. I have been fortunate to learn from him not only through all my topology classes at UNCC, but also through seminars, conferences, and our conversations. Without him, my research would not have been possible.

My sincere thanks goes to my committee members, professors Gabor Hetyei, Alan Dow, and Gamez Jose, for their insightful comments and questions. Professor Hetyei's knowledge and humor have enlightened my academic career. His expertise in graph theory has greatly guided my research. One of my goals in presenting a mathematical problem is to do it with such enthusiasm like professor Hetyei has always done.

I am also indebted to every other professor who has taught me: from the department of mathematics and statistics - professors Kevin McGoff, Loc Nguyen, Eliana Christou, Zhiyi Zhang, Evan Houston; from the department of computer science - professors Zbigniew Ras, Srinivas Akella, and Harini Ramaprasad. I thank Emeritus professor Bruno Wichnoski for his friendship and for sharing his knowledge in mathematical physics. "If I can see further, it is by standing on the shoulders of Giants". [Bernard of Chartres]

Last but not least, I would like to thank the department of mathematics and statistics, especially professor Shaozhong Deng, for having guided my academic career and supported me as a graduate teaching assistant. I also thank the graduate school for enabling my education, supporting me financially throughout the years, and finally all my graduate fellows for their friendship and discussion.

TABLE OF CONTENTS

LIST OF TABLES

LIST OF FIGURES

PREFACE

The formal study of knots and links started with Peter Tait in an effort to help his colleague, a physicist, Sir William Thomson, in vortex theory of atom which hypothesized that an atom was a vortex in the aether. Tait classified knots up to 10 crossings and started the branch of topology called knot theory.

A major problem in topology is to distinguish objects, hence the need for invariants. This dissertation proposes new link invariants and studies how it can be used to solve new problems.

CHAPTER 1: INTRODUCTION AND BACKGROUND

This chapter gives the background and defines terminologies for this dissertation. Interested readers may refer to any textbooks, such as [2], [3], [1], and [4] for basic knot theory knowledge and [5] for basic graph theory knowledge. For the dissertation to be self-contained, we define multiple terms and concepts below.

1.1 Knot Theory Basics

Definition 1.1.1. A *link of n components* is a subset of $\mathbb{R}^3$ that consists of n disjoint simple closed curves. A link with one component is called a knot.

In knot theory, we usually restrict ourselves to the so called "tamed links". In a tame link, each closed curve must satisfy certain regulatory conditions. For the purpose of this dissertation, we assume each component is a piecewise smooth curve.

The mapping $f : X \to Y$ is called an *embedding* if $f : X \to f(X)$ is a homeomorphism. That is, f is a continuous bijection and f^{-1} is also continuous. An embedding is *proper* if $f(\partial X) = f(X) \cap \partial Y$ and f(X) is not tangent to ∂Y, the boundary of Y.

Definition 1.1.2. Two embeddings f_0 and f_1 are *ambient isotopic* if there exists an isotopy $H : Y \times [0, 1] \to Y \times [0, 1]$ such that,

- $H(y, t) = (h_t(y), t)$. For each value of $t \in [0, 1]$, $h_t : Y \to Y$ is an orientation preserving homeomorphism;
- h_0 is the identity map;
- and $f_1 = h_1(f_0)$.

In [4], the author describes ambient isotopy as to fill Y with liquid and transport an object $(f_t(X))$ through it so that the object is moved along with the liquid.

Each equivalence class of links that are ambient isotopic to each other is called a *link type*. A classical problem of knot theory is to classify links with regards to equivalence.

Definition 1.1.3. A *link diagram* D is a projection of a link L into $\mathbb{R}^2$. In the diagram, we use the over and under information at a crossing to correspondingly refer to the overpasses and underpasses in $L \in \mathbb{R}^3$.

Definition 1.1.4. A projection p of a link L is called *regular* if p satisfies both of the following:

- The number of multiple points P_i are finite, and all multiple points are double points, meaning that $p^{-1}(P_i)$ contains two points of L.
- No vertex of L is mapped into a double point.

These double points mentioned in Definition 1.1.4 are called crossings of a link diagram of L. A crossing in D is assigned a positive or negative sign accordingly to the rule shown in Figure 1.1. The minimum number of double points (or crossings) in a projection of a link L over all possible regular projections is an intrinsic quantity of L that we shall discuss in Example 2.0.3.

Figure 1.1: Left to right: a double point where the under or over information is not specified, a positive crossing, and a negative crossing.

In this dissertation, a link projection D means a regular projection. It is an important result that almost all projections of piecewise linear smooth lines are regular. In other words, every link admits a regular projection. This can be seen if we consider the link a polygonal K on a plane P, then we can make P regular for K by arbitrarily perturbations of either K or P [1].

Definition 1.1.5. A link is said to be *positive/negative* if it admits a diagram D in which all crossings of D are positive/negative.

If we perform a crossing change (overpass to underpass or vice versa) to every crossing of a diagram D of a link L, then we obtain a diagram D' of the *mirror image* of L. If D is a negative diagram, then D' is positive.

Definition 1.1.6. A *2-tangle* T is a proper embedding of the disjoint union of 2 piecewise smooth arcs into a 3-ball.

A 2-tangle diagram, or a tangle diagram for short, is a regular projection of the 2-tangle into a plane, where the boundary of the 3-ball is projected into a circle. Two tangles T_1 and T_2 are equivalent if there exists an isotopy from T_1 to T_2 that keeps the end points of T_1 point-wise fixed.

A 2-tangle can have either parallel orientation or anti-parallel orientation, as shown in Figure 1.2.

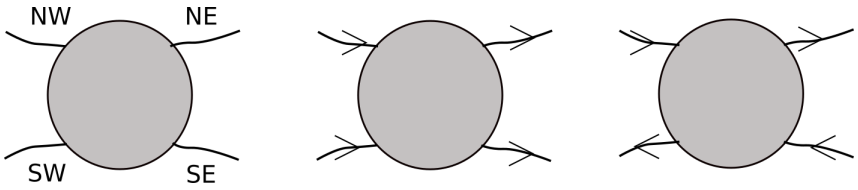

Figure 1.2: The 4 arcs in a 2-tangle. Tangle orientations: parallel - the arrows are pointing to the same direction, antiparallel - the arrows are in opposite directions.

Tangle parities are illustrated in Figure 1.3, which are categorized on only how the 2 strands position themselves with respect to 4 exits (SE, SW, NE, NW) of a 2-tangle. This differs from the parities that we will describe in Definition 4.2.4, which depends not only on the local structure of a tangle T, but also on the global structure of the diagram that contains T.

Definition 1.1.7. A *planar diagram (PD) code* of a link diagram D is a numerical representation of D in 4-tuples, obtained by numbering arcs with natural numbers in

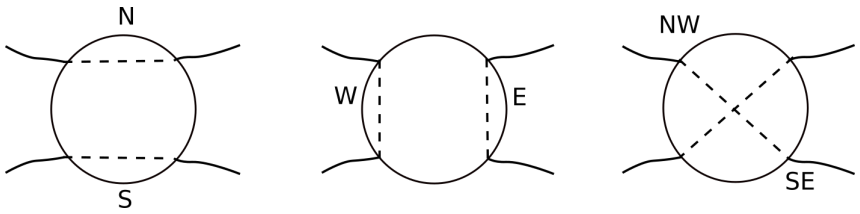

Figure 1.3: Parities of a 2-tangle. Left to right: parity 0, ∞, and 1.

an increasing order as one traverses each component. The order of the elements in the 4-tuples are determined by the arc labels (numbers) around each crossing, starting from the incoming lower arc following counterclockwise direction.

Figure 1.4 shows an example of a PD codes of the tabulated diagram of the figure-eight knot. In a link diagram, the order of traversing is arbitrary.

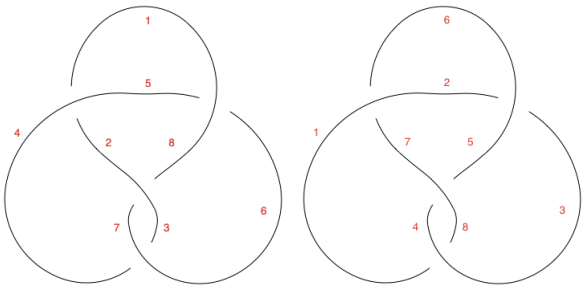

Figure 1.4: PD codes of the diagram D_1 on the left are: X[1, 4, 2, 5], X[3, 7, 4, 6], X[5, 8, 6, 1], X[7, 3, 8, 2], where X represents a crossing of D.

Since the choice of arc to start the numbering and the orientation of the link diagram is arbitrary, an n crossing link diagram can have $4n$ different PD-code representations. For example, the diagram D_2 on the right of Figure 1.4 gives a different set of 4-tuples, as follows X[6, 1, 7, 2], X[2, 5, 3, 6], X[8, 4, 1, 3], X[4, 8, 5, 7].

The PD codes used in this dissertation are from a Mathematica package, *knottheory*. We note that in [6], the author showed an explicit algorithm to reconstruct a well-defined link diagram on an orientable surface.

Below, we state a property of PD codes that is used in Chapter 7.

Remark 1.1.8. Definition 1.1.7 implies that each quadruple $[q_1, q_2, q_3, q_4]$ of PD codes of a link diagram contains a pair of even and a pair of odd numbers, such that they form two pairs of consecutive numbers. We note that the last arc numbered $4n$ is considered preceding the arc numbered 1, as one finishes traversing a component right before the starting arc. In addition, the signs of crossings are determined as follows:

1. A crossing is negative if the consecutive pairs appear in the same order (that is, both i and j appear before $i+1$ and $j+1$). For example, $[q_1 = i, q_2 = j, q_3 = i+1, q_4 = j+1]$.

2. A crossing is positive if the consecutive pairs appear in different order. For example, $[q_1 = i+1, q_2 = j, q_3 = i, q_4 = j+1]$.

1.2 Graph Theory Basics

Definition 1.2.1. *A graph* $G(V, E, r)$ is a triple consisting of a vertex set $V(G)$, and edge set $E(G)$, and a relation r that associates with each edge two vertices (which may or may not be distinct). The relation r is often implied in graph representations and thus, omitted in the notation.

A graph can be represented by a set of points and arcs in $\mathbb{R}^3$ in the following way:

- Each vertex $v \in V(G)$ is represented by a point in $\mathbb{R}^3$
- Each edge $e \in E(G)$ is represented by an arc in $\mathbb{R}^3$ such that its end points are the vertices that e is associated with according to the relation r.

Furthermore, two distinct edges do not intersect each other except at their endpoints in the case that edges connect to the same vertex (or vertices). If both endpoints of an edge connect to the same vertex, then the edge is called a *loop edge*. *Multiple edges* are edges sharing the same pair of endpoints.

Let u and v be the endpoints of an edge. Then, u and v are said to be *adjacent*. Two edges sharing the same vertex are said to be *incident* to each other. The adjective

"incident" is also used to describe a vertex v and an edge e such that v is an endpoint of e.

Definition 1.2.2. The number of edges incident to a vertex v_0 is the called the *degree* of v_0. If graph G contains only vertices of degree k, then G is said to have degree k.

For example, an even-degree graph G has all vertices of only even degree(s).

A *simple graph* is a graph that does not contain any loop edge or and any two distinct vertices can be connected by at most one edge.

A *multigraph* G' is a graph that is not simple. In this dissertation, we will consider graphs which are free of loop edges. A multigraph G' can be represented by an edge weighted simple graph, where the weight of an edge e is the number of edges between the two endpoints of e in the multigraph.

A connected graph G is a graph such that there is a path from any point to any other point in the graph. A *vertex cut* S is a subset of $V(G)$ such that $G - S$ has more than one connected component. A vertex cut of size 1 is called a *cut vertex*.

An *independent set* in a graph G is a set of pairwise nonadjacent vertices.

Definition 1.2.3. A *planar graph* is a graph that admits a representation on a plane such that edges meet only at vertices.

A graph G that is drawn in the plane without edges crossing is an embedding of G in the plane.

Let H be a subgraph of a graph G, that is, the vertex set and edge set of H are subsets of the vertex set and edge set of G, respectively. We say that H is an *induced subgraph* of G if H has the property that if two vertices v_1, v_2 are in H, then all the edges of G connecting v_1 and v_2 also belong to the edge set of H.

Definition 1.2.4. Let B be an induced and connected subgraph of G. We say that B is a *block* of G if B contains no cut vertices and is maximal in the sense that if there

is another induced and connected subgraph B' of G that contains no cut vertices, and B is a subgraph of B', then $B = B'$.

Definition 1.2.5. A *cycle* of a simple graph G is a sequence of distinct vertices $v_1, v_2, ..., v_k$ and a sequence of distinct edges $e_1, e_2, ..., e_k$ such that v_i and v_{i+1} are connected by e_i, for $1 \leq i \leq k$ and $v_{k+1} = v_1$.

Definition 1.2.6. A connected graph without any cycles is called a *tree*.

The *length* of a cycle is the number of edges in the cycle.

Definition 1.2.7. The *circumference of a graph* G is the length of the longest cycle in G.

Definition 1.2.8. A graph G is said to be *Hamiltonian* if G contains a Hamiltonian cycle, that is, a cycle that contains all vertices of G.

Definition 1.2.9. *A graph G is said to be bipartite if the set of vertices of G is the union of two disjoint independent sets U and W, which are called partite sets of G.*

Definition 1.2.9 means that every edge of G must connect a vertex in U with a vertex in V. In other words, no two vertices within U or V are adjacent. Since we are interested in graphs that are not only Hamiltonian, but also bipartite. The following result relates these two properties of a graph by stating a condition for a bipartite graph to be Hamiltonian.

Proposition 1.2.10. *Let a connected and simple graph G be bipartite with partite sets U and W. If G is also Hamiltonian, then the size of U and W must be the same.*

Proof. Let the size of U be u and the size of W be w. Without loss of generality, we suppose that $u > w$. Since G is also Hamiltonian, let $v_1...v_kv_1$ be a Hamiltonian cycle of G, for some k, that starts at $v_1 \in W$. We visit v_1 the second time after traversing $2w$ edges and after visiting all vertices of W. But we have not visited all vertices of G

by traversing this Hamiltonian cycle $v_1...v_kv_1$ of G: the number of left out vertices is precisely $u - w$. This contradicts the hypothesis that $v_1...v_kv_1$ is a Hamiltonian cycle of G, hence Proposition 1.2.10 follows. □

Definition 1.2.11. In a graph G, the set $\mathbb{C}$ of cycles that can generate every cycle in G by a linear combination of the elements in $\mathbb{C}$ is called the *cycle basis* of G. In other words, $\mathbb{C}$ is a maximal linearly independent set of cycles of G.

Proposition 1.2.12. *Let $G(V, E)$ be a plane graph. Then the number of basis cycles of G is given by $|E| - |V| + 1$.*

A well-known result characterizes bipartite graphs in terms of their cycle lengths. Interested readers can refer to [7] for a proof of Proposition 1.2.13, which essentially shows that a cycle with odd length cannot have vertices colored so that no two adjacency vertices are of the same colors, by using only 2 colors.

Proposition 1.2.13. [7] *G is bipartite if and only G contains no cycle of odd length.*

Definition 1.2.14. The *adjacency matrix* $\mathbb{M}(G)$ of a graph G of n vertices is a square $n \times n$ matrix that represents the graph G as follows: the row headers and column headers are marked with vertices $v_1, ..., v_n$. Each element of $\mathbb{M}$ represents the number of edges between any two vertices v_i and v_j in G. For a loop-free graph, all diagonal entries are zero.

In this dissertation, we use adjacency matrices to represent Seifert graphs (described in Definition 4.2.1) in the computation of writhe-like invariants. The signs of each element of $\mathbb{M}$ represents the crossing sign in the original link diagram D.

Lemma 1.2.15. *Let B be a block of a bipartite graph G, then B can only be one of the following three types of subgraphs of G: (i) B consists of an isolated vertex of G; (ii) B consists of two cut vertices of G and all the edges between them, and (iii) every edge of B belongs to a cycle of length at least 4 in B.*

Proof. If B contains an isolated vertex of G, the maximal condition is satisfied and B is a block of G. Let B' the edge weighted simple graph obtained from B.

If B' is a single edge graph with vertices v_1 and v_2 and this edge is a bridge edge of G then B' must be a block. To see this we only need to show that it is maximal since it obviously does not contain any cut vertices of its own. If it is not maximal, then there exists a block B_1 that contains it as a proper subgraph. This is impossible since at least one of v_1 and v_2 would be a cut vertex of B_1.

If B' is not a single edge graph then let us consider an edge $e \in E(B')$. Let v_1, v_2 be the end vertices of e. We note that B' is a simple graph and it is free of cut vertices. By the assumption, B' has at least one more vertex v_3. It is a well-known fact that a simple graph with three or more vertices is free of cut vertices if and only if every edge in it belongs to a cycle. Thus e belongs a cycle in B' with an even length at least 4 since B' is also bipartite. □

A plane graph can be regarded as a one dimensional topological space. It is possible that two plane graphs are isomorphic as graphs, but are not equivalent topologically. For example, the mirror image of a plane graph (using any straight line in the plane as the line of reflection) may not be topologically equivalent to itself.

In [8], Whitney introduced and studied a graph operation called Whitney flip. In this paper we will use several similar operations, which are defined below.

Definition 1.2.16. Let $\{v_1, v_2\}$ be a 2-cut of a plane graph G and let H be an induced and connected subgraph of G that is $\{v_1, v_2\}$-dependent. Let H' be the mirror image of H with v_1' and v_2' being its vertices corresponding to v_1 and v_2. In the case that v_1 and v_2 are connected by an edge e, then a *Type A Whitney flip* is the operation that attaches H' to $G \setminus H$ by identifying v_1' to v_2 and v_2' to v_1 as shown in Figure 1.5.

Definition 1.2.17. Let v_1, v_2 be two vertices of a plane graph G that are connected by a single edge e. Let H be an induced and connected subgraph of G that is v_1-

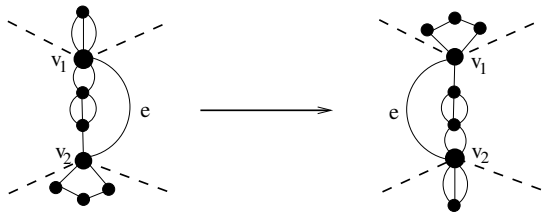

Figure 1.5: An example of Type A Whitney flip.

dependent. The operation that attaches its mirror image H' to $G \setminus H$ by identifying v_1' (the vertex in H' corresponding to v_1) to v_2 while keeping e intact is called a *Type B Whitney flip*. An example is shown in Figure 1.6.

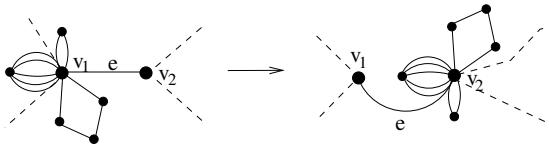

Figure 1.6: An example of Type B Whitney Flip.

Definition 1.2.18. Let v_0, v_1, v_2 be three vertices of a plane graph G such that there is a single edge e between v_0, v_2 and v_1 is a 1-cut of $G - e$. Let H be an induced and connected subgraph of G that is v_1-dependent in $G - e$ and let H' be the mirror image of H with v_0', v_1' being its vertices corresponding to v_0 and v_1. The operation that attaches H' to $G \setminus H$ by identifying v_0' to v_2, v_1' to v_0, and moves the edge e to be between v_0 and v_1 is called a *Type C Whitney flip*. An example is shown in Figure 1.7.

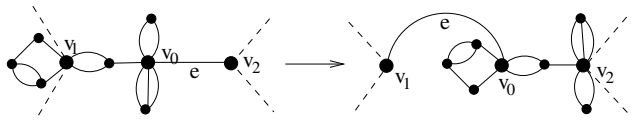

Figure 1.7: An example of Type C Whitney Flip.

Definition 1.2.19. Let v_0, v_1 be 2 vertices of a plane graph G with at least an edge e connecting them. Let H be an induced and connected subgraph of G containing v_0, v_1 such that H is v_1-dependent. Let H' be the mirror image of H with v_0' being the mirror of v_0 in H'. Then a *Type D Whitney flip* is the operation that attaches H' to $G \setminus H$ by identifying v_0' to v_1 as shown in Figure 1.8.

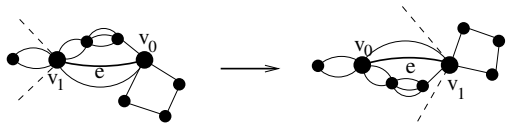

Figure 1.8: An example of Type D Whitney Flip.

Remark 1.2.20. In this dissertation, we will only consider graphs without single bridge edges. Thus we are only interested in what the Whitney flips defined above can do to such a graph. We observe that a Whitney flip of Type A or B can only move a block of G attached to one cut vertex to another cut vertex without changing the internal structure of the block. On the other hand, a Whitney flip of Type C can only be applied to a block B that has a singular necklace decomposition and must use a bead H' that is a single edge graph as the edge e in the definition of the flip. The flip exchanges the position of e and a chain of beads (one or more consecutive beads, that is). Some blocks attached to cut vertices that belong to either this chain of beads or H' may be moved to another terminal without internal structure change as the by-product of this flip without any internal structural change.

Definition 1.2.21. Let H be a block of G. We say that H admits a *necklace decomposition* if there exist a set of vertices $\{v_1, v_2, ..., v_k\} \subset V(H)$ $(k \geq 2)$ and induced subgraphs H_1, ..., H_k of H such that the following are satisfied:

(i) $E(H_i) \cap E(H_j) = \emptyset$ if $i \neq j$, $1 \leq i, j \leq k$;

(ii) $E(H) = \cup_{1 \leq j \leq k} E(H_j)$;

(iii) $V(H_i) \cap V(H_{i+1}) = \{v_{i+1}\}$ for $1 \leq i \leq k-1$, $V(H_k) \cap V(H_1) = \{v_1\}$, and $V(H_i) \cap V(H_j) = \emptyset$ for all other H_i, H_j pairs;

(iv) The set $\{v_1, v_2, ..., v_k\}$ is maximal in the sense that if there exist another set of vertices $\{v'_1, v'_2, ..., v'_{k'}\} \subset V(H)$ and induced subgraphs H'_1, ..., $H'_{k'}$ of H satisfying conditions (i) to (iii), and

(v) $\{v_1, v_2, ..., v_k\} \subset \{v'_1, v'_2, ..., v'_{k'}\}$. Then we must have $\{v_1, v_2, ..., v_k\} = \{v'_1, v'_2, ..., v'_{k'}\}$ (and consequently $k' = k$, $H_j = H'_j$ for all j).

Each H_j in Definition 1.2.21 is called a *bead*, and the two vertices v_j, v_{j+1} are called the terminals of the bead H_j.

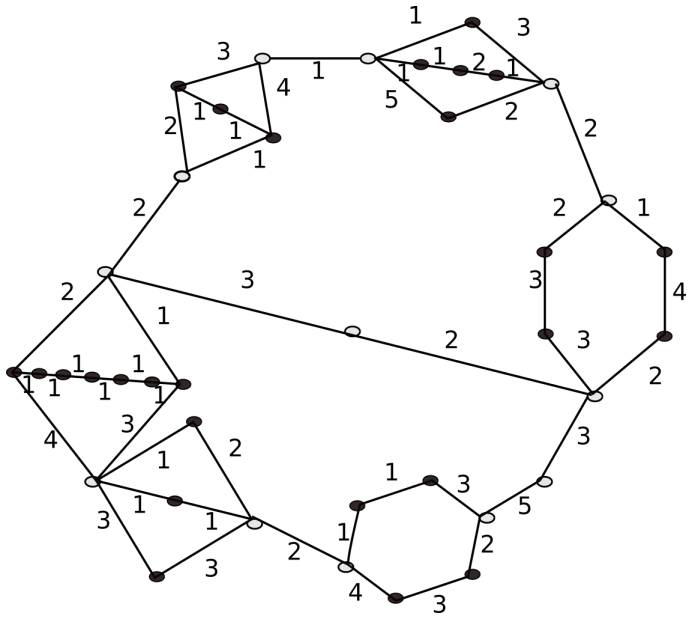

Figure 1.9: The graph G admits a necklace decomposition.

CHAPTER 2: LINK INVARIANTS

Definition 2.0.1. A link invariant I is a quantity $I(L)$ assigned to a link L, such that if L_1 is equivalent to L_2, then $I(L_1) = I(L_2)$.

If $I(L_1) \neq I(L_2)$, then L_1 and L_2 must be of different link types. Whether the link types of L_1 and L_2 are the same or not is indecisive if $I(L_1) = I(L_2)$.

To reduce the topological problem of whether two links are ambient isotopic to a diagrammatic problem, we use Reidemeister moves, as described below.

Definition 2.0.2. A Reidemeister move (R-move) is an operation on a diagram of a link that does not alter the type of the corresponding link. There are 3 types of R-moves:

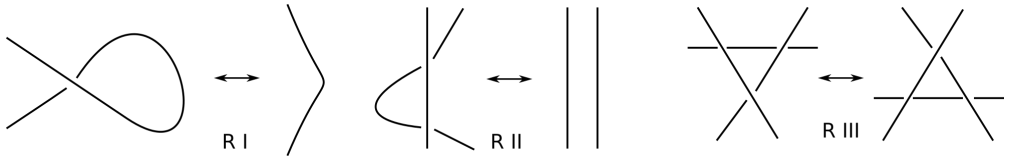

Figure 2.1: Left to right: Reidemeister moves I, II and III (abbreviated as R-I, R-II, and R-III).

There are generally two types of link invariants:

- one that is defined over all possible projections of the link as in Example 2.0.3, 2.0.5, and Definition 2.0.7.
- one that is defined based on any given diagram of a link, as in Examples 2.0.12 and 2.0.8.

Example 2.0.3. *The crossing number of a link L_1 is the minimum number of crossings over all possible configurations of L_1. Figure 2.2 shows 2 configurations of the trefoil, only one of which has 3 crossings.*

It is trivial to see that the number of crossings obtained from a single diagram of a link is not a link invariant, since the Reidemeister moves of Type I and Type II dot not preserve the number of crossings in the diagram. The (minimum) crossing number, as defined in this Example 2.0.3, is used for categorizing knots and links. However, by its definition, it is difficult to compute when given an arbitrary link diagram, since we have no general methods to determine whether the number of crossings in the diagram can be reduced or not.

Figure 2.2: A diagram of the knot 3_1 with minimal number of crossings 3, and a non-minimal diagram of the same knot.

A surface F is called *orientable* if every point in F can be associated consistently with a direction of either clockwise or counterclockwise. Figure 2.3 illustrates a diagram of an orientable surface in comparison with one of a non-orientable surface. We are not concerned about nonorientability in this dissertation.

Definition 2.0.4. A Seifert surface F of a link L is an orientable surface whose boundary is the link L.

The fact that every link bounds an orientable surface is guaranteed by a well-known algorithm introduced and proved by Herbert Seifert [9]. We will describe this algorithm in Chapter 4.

Figure 2.3: Left: the surface of a torus is orientable. Right: the surface of a Mobius band is non-orientable.

A *Seifert surface* for a link L is an orientable surface such that the boundary component(s) of the surface is (are) the link L.

Example 2.0.5. *The genus of a link L, $g(L)$, is the minimal genus of all orientable surfaces whose boundary is the link L.*

For example, the unknot bounds a disc and $g(unknot) = 0$, illustrated in Figure 4.2.

In [3], a *cylindrical n-tangle* is defined as a ball $D^2 \times [0, 1]$ with a line of n inputs in the top $D^2 \times 1$ and a line of an outputs directly below them at the bottom.

Definition 2.0.6. An n-string braid is a cylindrical n-tangle such that all n strings descend monotonically everywhere.

We often use a 2-dimensional projection of this n-tangle, as illustrated in Figure 2.4 on the left, with an open 3-braid, where all strings hang from the top bar, crossing under or over other strings while (only) dropping to the bottom bar. It is also common to see an open braid that is a 90° rotation of the braid on the left of Figure 2.4. When corresponding ends of the n strings are connected in pairs, we have a closed braid. The fact that every link can be represented by a closed braid [10] gives rise to the invariant in Definition 2.0.7.

Definition 2.0.7. A braid index $br(L)$ of a link L is the least number of strings needed to make a closed braid presentation of a link.

We note that the value of $br(L)$ is the minimizer of a geometric property over all possible diagrams of the link L; thus, it is independent of projections of L and is hard to determine. A classical result [11] stated in Chapter 4 relates the braid index of a link L with the number of discs in the Seifert surface of a projection D of L. Recently, there has been progress in the determination of braid index for reduced alternating links in general [12], for special families of links like the Montesinos links [13] in particular.

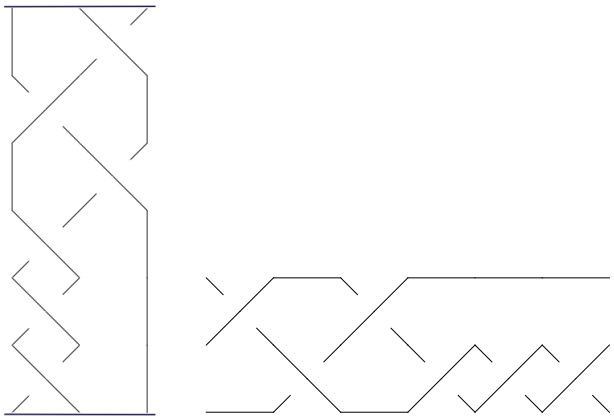

Figure 2.4: Left: an open 3-braid. Right: another presentation of the same open 3-braid.

Example 2.0.8. *Let $c_1, c_2, ..., c_n$ be the n crossings of a link L. The linking number lk of a 2-component link L (with K_1, K_2 being the two components) is defined as $lk(K_1, K_2) = \frac{1}{2}(sign(c_1) + sign(c_2) + ... + sign(c_n))$, where the c_i's are all crossings between K_1 and K_2.*

The linking number describes how components intertwine around each other in a 2-component link. So this invariant is specific to a link diagram, up to its orientation. We can easily see that lk is an invariant by consider the effects of Reidemeister moves on lk. Moreover, the value of lk is always an integer. This can be seen by observing that a curve must enter and exit another curve in order to make a link. In other words, the Jordan curve theorem guarantees that the sum of signs of all crossings

between 2 components of a link is even, hence half of this sum is an integer.

Figure 2.5 shows an example of a splittable link L_1 with $lk(L_1)$=0, and a Hopf link L_2 with the linking number of 1 and the other with linking number -1.

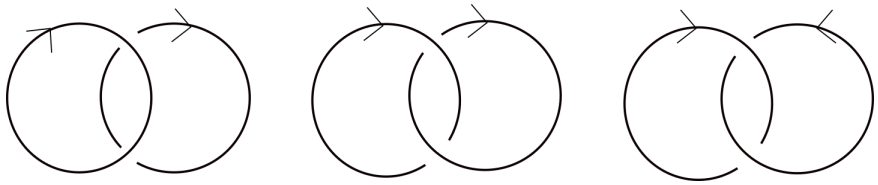

Figure 2.5: Left: $lk(L_1) = \frac{1}{2}(1-1) = 0$. Middle: $lk(L_2 = \frac{1}{2}(1+1) = 1$. Right: $lk(L_2 = \frac{1}{2}(-1-1) = -1$.

It is well known that two diagrams of links are isotopic if and only if one can be transformed to the other by a finite sequence of R-moves [14].

We consider how linking number is changed when an R-move of any type is performed.

R-I move involves only one component of a link diagram, so the value ± 1 does not contribute to $lk(D)$.

Figure 2.6 shows the case of R-II. By symmetry, we have only 2 combinations for the orientation of the two strands; either their orientations are both pointing towards the crossings, or only one is pointing towards the crossings. In both cases as shown in Figure 2.6, the crossings always have opposite signs. Thus, the total net change in signs is $-1+1=0$ and $1-1=0$.

In the case of R-III, as illustrated in Figure 2.7, the circled crossing O is not affected by the move, no matter how D is oriented; meanwhile the two crossings created or destroyed by sliding one strand over O the yield the same signs before sliding as after sliding. The argument holds for different orientations of the three strands in Figure 2.7.

An example of an invariant that can be powerful, yet not as hard to compute as

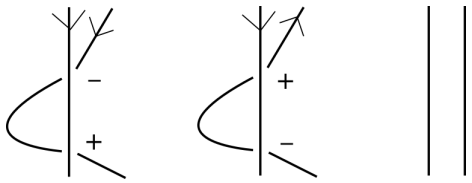

Figure 2.6: Net change in signs of R-II.

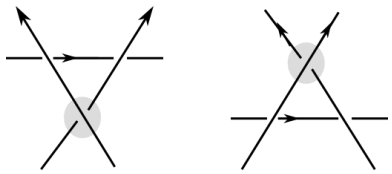

Figure 2.7: The effect of R-III on signs.

minimum quantities among all possible link configurations, is a knot polynomial. A well-known knot polynomial was discovered by Jones Vaughan in 1985 [15]. Subsequently, another notable mathematician, introduced the bracket polynomial (Definition 2.0.9) which was a model to interpret Jones polynomial [16]. Below, we will use the bracket polynomial approach to define Jones polynomial.

Definition 2.0.9. The bracket polynomial $\langle D \rangle$, of any unoriented link diagram D is a polynomial in one variable A defined by the recursive rules:

$$\langle \times \rangle = A\langle \)\(\rangle + A^{-1}\langle \asymp \rangle,$$

$$\langle \times \rangle = A\langle \asymp \rangle + A^{-1}\langle \)\(\rangle,$$

$$\langle \bigcirc L \rangle = -(A^2 + A^{-2})\langle L \rangle,$$

$$\langle \bigcirc \rangle = 1.$$

Conventionally, by link invariant, we mean that it is a general invariant, under ambient isotopy. To discretize the equivalence, we use R-moves. However, there exists restricted invariants that apply only to special families of links, or under R-II

Figure 2.8: The writhe values of the two diagrams are different.

and R-III moves only. The bracket polynomial in Definition 2.0.9 is an example of a link invariant under R-III and R-IIII moves, or regular isotopy. Another example of an invariant under regular isotopy is illustrated in Example 2.0.10.

Example 2.0.10. *The writhe $\omega(D)$ of a link diagram D is a quantity defined by the difference of the total number of positive crossings minus the total number of negative crossings.*

Figure 2.8 shows that R-I can change the writhe of a diagram by ± 1.

Proposition 2.0.11. [16] *The one variable bracket polynomial in Definition 2.0.9 is invariant under R-II and R-III moves.*

We will show one case of Proposition 2.0.11 by showing that the bracket of both R-II configurations are equal: $\langle$ $\rangle = \langle$ $\rangle$.

$$\begin{aligned}
\langle \text{  } \rangle &= A\langle \text{  } \rangle + A^{-1}\langle \text{  } \rangle \\
&= A(A\langle \text{  } \rangle + A^{-1}\langle \text{  } \rangle) + A^{-1}(A\langle \text{  } \rangle + A^{-1}\langle \text{  } \rangle) \\
&= A(A\langle \text{} \rangle + A^{-1}((-A^2 - A^{-2})\langle \text{} \rangle)) + A^{-1}(A\langle \text{  } \rangle + A^{-1}\langle \text{} \rangle) \\
&= A^2\langle \text{} \rangle - A^2\langle \text{} \rangle - A^{-2}\langle \text{} \rangle + \langle \text{} \rangle + A^{-2}\langle \text{} \rangle \\
&= \langle \text{} \rangle = \langle \text{} \rangle.
\end{aligned}$$

Similarly, it can be shown that $\langle$ $\rangle = \langle$ $\rangle$ and $\langle$ $\rangle = \langle$ $\rangle$.

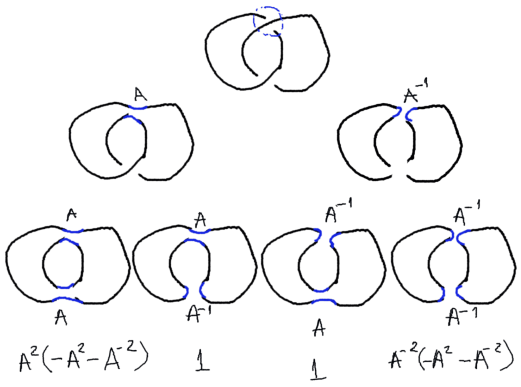

Figure 2.9: The bracket polynomial of the Holf link diagram above is given by: $-A^4 - A^{-4}$.

However, $\langle \times\!\bigcirc \rangle = -A^3\langle \;) \; \rangle$, and $\langle \times\!\bigcirc \rangle = -A^{-3}\langle \;) \; \rangle$. That is to say the bracket polynomial is not invariant under R-I move. In [16], the author shows a general link invariant (Definition 2.0.12) can be formed by normalizing the bracket polynomial.

Definition 2.0.12. Let $\omega(D)$ be the writhe of a link diagram D, and $\langle D \rangle$ is the bracket polynomial of D, then the *Kauffman polynomial* X in variable A is given below:

$$f(D) = (-A)^{-3\omega(D)}\langle D \rangle.$$

From Definition 2.0.12, by substituting the variable A in $f(L)$ with $t^{-1/4}$, one gets the Jones Polynomial:

$$V(L) = (-t)^{\frac{3}{4}\omega(L)}\langle L \rangle.$$

Figure 2.9 gives an example of the bracket polynomial of a Holf-link diagram, from which the Jones polynomial can be given as,

$$V(L) = -\sqrt{t} - t^{5/2}.$$

Even though computing polynomial invariants is easier than minimizing quantities over all possible configurations, the task is still challenging in terms of computa-

tion complexity. In Chapter 7, we will discuss further how hard it is to calculate a Kauffman polynomial and Jones polynomial.

CHAPTER 3: THE FLYPE CONJECTURE

Definition 3.0.1. *An alternating link L is a link that possesses a regular projection into $\mathbb{R}^2$ with alternating overpasses and underpasses.*

Definition 3.0.2. *A link diagram is reduced if it contains no nugatory crossing.*

Figure 3.1: A nugatory crossing can be undone by untwisting the crossing. The gray circles suggest that any structure of a link can be on both sides of the nugatory crossing.

Definition 3.0.3. *A flype is a local move on a link diagram that rotates a tangle T 180 degrees, such that a single crossing is flipped from one side of the tangle to the other side, as shown in Figure 3.2.*

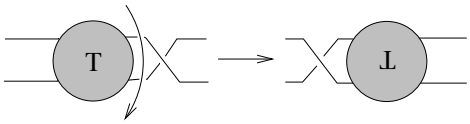

Figure 3.2: A flype on the tangle T.

Theorem 3.0.4 [17] settled the 100-year-old Tait Flyping Conjecture at the time, which allowed the authors to complete the classification of alternating links [18].

Theorem 3.0.4. *Given two reduced alternating diagrams, they are of the same type if and only if they are related by a sequence of flypes.*

Since a flype does not change the writhe, Theorem 3.0.4 implies that writhe is a link invariant if we restrict ourselves to reduced alternating link diagrams. In general the writhe of a link diagram is not an invariant in the equivalence class induced by all Reidemeister moves, because a type I Reidemeister move changes the writhe by $+1$ or -1. It is still not an invariant even if we restrict ourselves to minimal link diagrams. A well known example is the Perko pair consisting of knots 10_{161} and 10_{162} enumerated in Rolfsen's knot table [1].

CHAPTER 4: SEIFERT DECOMPOSITION AND SEIFERT GRAPHS

4.1 Seifert Decomposition

A combinatorial representation of an oriented link diagram D can be obtained by smoothing all the crossings in the diagram as shown in Figure 4.1. Then, all resulting partial arcs are connected, which forms closed curves that we call Seifert circles (or s-circles). The result is a Seifert diagram that includes Seifert circles and the crossings that have been smoothed. We call this process the Seifert circle decomposition $S(D)$ of the oriented link diagram D.

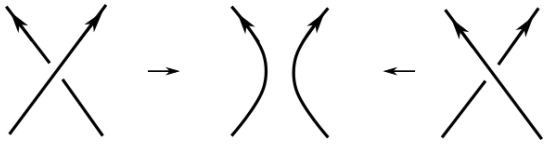

Figure 4.1: Smooth a (positive/negative) crossing.

We note that $S(D)$ gives the construction of the Seifert surface of D mentioned in Definition 2.0.4, by replacing s-circles with discs in different heights and connecting these discs with twisted bands where the crossings of D are.

Proposition 4.1.1 relates the number of s-circles to the listed quantities in a Seifert surface whose boundary admits the diagram D.

Proposition 4.1.1. *The genus of a Seifert surface F constructed from a connected μ-component link diagram D satisfies:*

$$2g(F) = 2 + c(D) - s(D) - \mu,$$

where $s(D)$ is the number of s-circles in $S(D)$ and D is the boundary of F, $c(D)$ is

the crossing number of D.

We note that if link L is homogeneous, then the surface F above yields the minimal genus $g(L)$ of the link L. That is, $g(F) = g(L)$ [19].

For example, the unknot bounds a disc. The surface F whose boundary is the unknot in Figure 4.2 gives the unknot diagram D with $c(D) = 1$ and $\mu = 1$, and $S(D)$ gives $s(D) = 2$. Thus, $g(F) = 0$ and the genus of the unknot is 0.

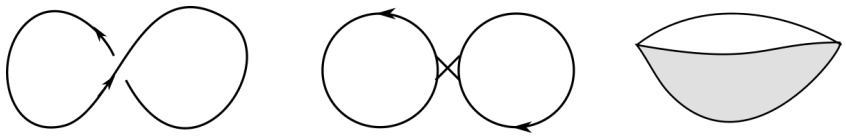

Figure 4.2: Left: a diagram D of the unknot. Middle: Seifert decomposition of D. Right: The surface F that the unknot bounds. If we cap F with a disc, we obtain a sphere (not shown), which has genus 0. We have $g(unknot) = g(F) = \frac{1}{2}(2+1-2-1) = 0$.

4.2 Properties of Seifert Graphs

Definition 4.2.1. *Let D be an oriented link diagram and $S(D)$ be its Seifert circle decomposition. We construct a graph $G_S(D)$ from $S(D)$ by identifying each Seifert circle to a vertex of $G_S(D)$. If there exist $k \geq 1$ crossings between two Seifert circles C_1 and C_2 in $s(D)$, then the two corresponding vertices v_1 and v_2 are connected by k edges. Otherwise, there does not exist an edge between the two vertices. $G_S(D)$ is called the* Seifert graph *of D.*

Using the same notation in Definition 4.2.1, $G_S(T)$, where T is a tangle in a diagram D, means the portion of the Seifert graph of D that we focus on is the local graph structure that corresponds to the tangle T in D.

The following is a well-known result by Yamada [11] that relates the number of s-circles to a link invariant.

Theorem 4.2.2. [11] *The minimum number of s-circles among all possible projections of a link L equals the braid index of L.*

Remark 4.2.3. Seifert graphs are planar. We will show this by construction. Starting with a link diagram D (which is a regular projection of a link on a plane P), smooth all crossings. The resulting s-circles left on P, categorized into only two types: those that are nested (a) and those that are not nested (b). We note that type (b) includes those that contain other s-circles inside. Since D is entirely on the plane P, all type (b) s-circles and the original crossings of the regular diagram D are also on P, it is evident that identifying all type (b) s-circles with vertices and crossings of D with edges results in a plane subgraph of $G_S(D)$. For type (a) s-circles, we start at the outermost circle c_1 that is contained by a type (b) circle c_0, and move c_1 to the same level with c_0 on the plane. When identifying c_1 with a vertex, and crossings between c_0 and c_1 with edges, we simply place these edges on P avoiding to cross other edges that are already on P. We repeat this step until there is no more type (a) s-circles. In Definition 4.2.5, we describe the nesting structure of s-circles in a precise language of levels.

Definition 4.2.4. Let T be a tangle in a link diagram D. We consider all possible scenarios of T after the Seifert decomposition of D. We say the Seifert decomposition of T has *parity hp* if T is decomposed into cases (i) or (iv), *parity ha* if cases (ii) or (iii), *parity vp* if cases (v) or (viii), and *parity va* if cases (vi) or (vii) respectively.

Tangle parities and the global structure of a link diagram affect how a tangle may look like after a Seifert decomposition. For example, a tangle of parity 1 can have any of the Seifert decomposition parities *hp*, *ha*, *vp*, or *va*.

Definition 4.2.5. *Let D be a connected diagram of an oriented link and consider the Seifert decomposition of D. If an s-circle C is not bounded within any other s-circle, then we say that C has level number 0 and we write this as $l(C) = 0$. If a Seifert circle C is bounded within a level* 0 *s-circle, but not bounded inside any other s-circles, then we say that it has level number -1 and we write this as $l(C) = -1$. Repeating*

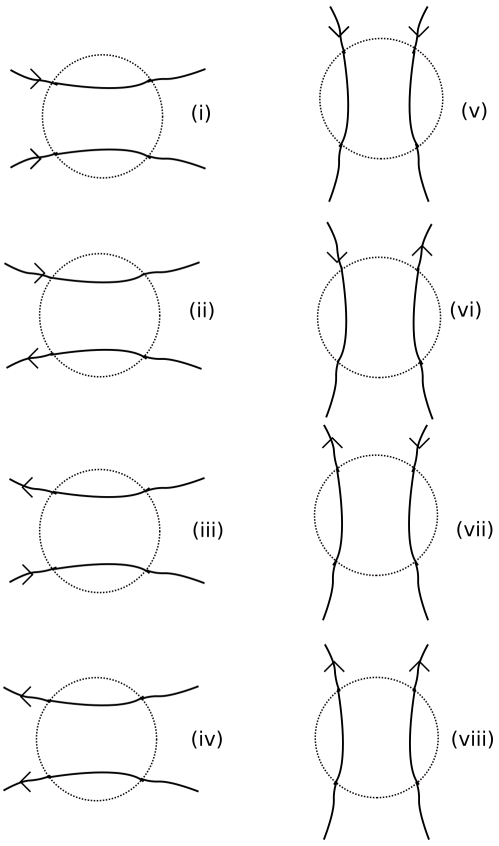

Figure 4.3: Seifert decomposition parities. We note that possible complete Seifert circles inside T are not drawn in Figure 4.3.

this process, the level number of any s-circle can be defined, recursively: assume that all s-circles of level $\geq -k$ *have been defined, then an s-circle* C *that is bounded within a level* $-k$ *s-circle is assigned a level number, i.e.* $l(C) = -k - 1$.

Consider the case when a level $-k+1$ s-circle bounds one or more level-k s-circles. Since the original diagram D (before $S(D)$) is connected, its Seifert diagram, and hence Seifert graph is also connected. We call the collection of these s-circles an *s-block* and k is the level number of the s-block, except for level 0: The collection of level 0 circles forms the level-0 s-block. If there is only one level-0 s-circle, then the 0-block contains only one s-circle. We will the same name for the counterpart of s-block in $G_S(D)$

Remark 4.2.6. It is easy to see that for any diagram D, its Seifert decomposition

has at least one level 0 s-circle. In other words, $G_S(D)$ has at least one vertex. When the level $-k+1$ s-circle bounds one or more level $-k$ s-circles, the collection of these s-circles gives an s-block with level number $-k$.

Remark 4.2.7. Seifert graphs are bipartite. If $\tilde{G}$ is a tree, it is evident to see that $\tilde{G}$ is bipartite by showing that $\tilde{G}$ is two-colorable; that is, vertices of $\tilde{G}$ can be colored alternately with exactly two colors. Pick a vertex v_0 of $\tilde{G}$ to be a root, and any other vertex v_i among the rest of the set of vertices of $\tilde{G}$. Color v_0 as black. Let l be the length of the path from v_0 to v_i; the existence and uniqueness of this path is guaranteed by the fact that G is a tree. If l is even, then color v_i the same color with the node (black); otherwise, color v_i white. The sets of black and white vertices bipartition of $\tilde{G}$.

In the case that $\tilde{G}$ contains a cycle γ, due to the orientations (clockwise and counterclockwise) of adjacent s-circles in the cycle, γ must contain an even number of vertices hence γ must have an even length. Then $\tilde{G}$ is bipartite by Theorem 1.2.9.

The term 'homogeneous links' was introduced by Cromwell in [19]. Alternating links and positive links are two special subclasses of homogeneous links, in which blocks of Seifert graphs of the former alternate between positive and negative signs while all blocks of Seifert graphs of the later have the same sign.

Definition 4.2.8. *An oriented link is homogeneous if it admits a homogeneous diagram D whose Seifert graph $G_S(D)$ is homogeneous; that is, within each block of $G_S(D)$, edges have the same sign.*

Remark 4.2.9. Since D is a reduced alternating link diagram, all crossings belonging to the same s-block of $G_S(D)$ have the same sign, and s-blocks whose level numbers differ by an odd integer contain crossings of different signs.

Remark 4.2.10. Let $s(D)$ be the size of the vertex set of $G_S(D)$, where D is a μ-component link diagram of $c(D)$ crossings. Then we have, $c(D)-s(D) \equiv \mu(\mod 2)$.

To show Remark 4.2.10, we first consider the case when the diagram D has no crossings, i.e. all s-circles of D are the components of D. So the statement $c(D) - s(D) \equiv \mu(\mod 2)$ holds.

When $c(D) = 1$, we have the situation as shown on the left of Figure 4.4, where the dash lines represent short arcs. After smoothing this crossing, μ is changed by $+1$ which gives $s(D) = 2$. So the statement also holds in the case the diagram D is reducible.

We suppose that the statement also holds for $c(D) = cr$, and $s(D)$ of a μ-component link diagram D. We consider the quantity $cr + 1 - s(D')$ in the μ-component link diagram D'. Smoothing this additional crossing in D' must increase (as shown on the left of Figure 4.4) or decrease (as shown on the right of Figure 4.4) the number of components of D' by 1, thus changes $s(D')$ by ± 1. We now consider the difference of $c(D')$ and $s(D')$ and apply the induction hypothesis.

1. In the case shown in Figure 4.4 on the left, we have $cr + 1 - s(D') = cr + 1 - (s(D') + 1) \equiv \mu(\mod 2)$.

2. In the case shown in Figure 4.4 on the right, we have $cr + 1 - s(D') = cr + 1 - (s(D') - 1) = cr - s(D') + 2 \equiv \mu(\mod 2)$.

Since we sometimes refer to the simple Seifert graph resulting from $S(D)$, we use $\tilde{G}_S(D)$ to mean the simple graph obtained from the multigraph $G_S(D)$ whose edges are assigned signed weights in the following way: the absolute value of the weight of an edge e connecting two vertices v_0 and v_1 in $\tilde{G}_S(D)$ is the total number of crossings between the s-circles of D that correspond to v_0 and v_1, and the sign of the weight of e is the sign of these crossings. By Remark 4.2.9, all edges belonging to the same block in $\tilde{G}_S(D)$ must have weights of the same sign. Since D is reduced (that is, it is free of nugatory crossings), $G_S(D)$ is free of bridge edges, which implies that $\tilde{G}_S(D)$ is free of bridge edges whose absolute weights equal to one. In addition, it worth

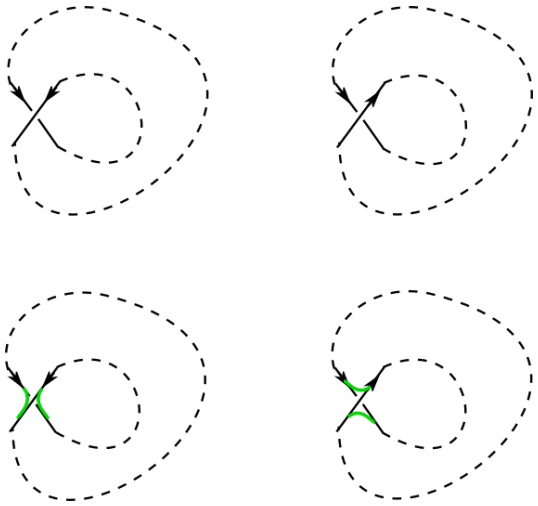

Figure 4.4: Smoothing a crossing increases or decreases the number of components by 1. The dash parts represent long arcs, whose self intersections are not drawn. Top: the crossings before smoothing. Bottom: the resulting closed curves after smoothing and joining the corresponding arcs.

noticing that if $G_S(D)$ is not a tree, then D must be a nontrivial diagram of a link, since a tree must be a simple graph. In [19], diagrams whose graphs $G_S(D)$ are trees were characterized throughout the homogeneous class of links as diagrams of trivial links.

CHAPTER 5: WRITHE-LIKE INVARIANTS OF REDUCED ALTERNATING LINKS

5.1 Whitney Flip Moves

We examine how flypes on reduced alternating link diagrams can affect their Seifert graphs. We first consider the case when two reduced alternating link diagrams $D1$ and $D2$ are related by a single flype move. Then, we generalize it for a finite sequence of flype moves. Let T be the tangle where the flype takes place. Without loss of generality, let us assume that we start with a diagram in which the crossing used for this flype move is on the right side of T as shown in Figure 3.2. There are eight possible combinations to consider depending on the orientations of the four strands that enter/exit T. All Seifert decomposition parities are given in Definition 4.2.4: which includes four pairs: hp, ha, vp, and va. By symmetry, we will need to consider only one of each pair listed in Definition 4.2.4 and Figure 4.3, which results in the four distinct scenarios shown in Figure 5.1. We note that in Figure 5.1, we focus only on the 4 strands that enter/exit T, and not what is inside T.

Now we consider the Seifert decomposition of the flype-related structure, $S(T)$, and illustrate each of the four cases by filling in T its Seifert diagram after crossings are smoothed. To simplify the language, we will relabel the cases hp, ha, va, vp as A, B, C, and D correspondingly, as illustrated in Figure 5.2.

In cases A, B, and C, because of their orientations, the two Seifert circles C_1 and C_2 (defined by the two parallel arcs entering/exiting T after all crossings are smoothed) must be distinct from each other and remain in both $S(D_1)$ and $S(D_2)$.

Case A: A flype moves the crossing O to the left side of the tangle and the other structure in $T \cap S(D_2)$ is obtained from $T \cap S(D_1)$ by an 180 degree rotation around

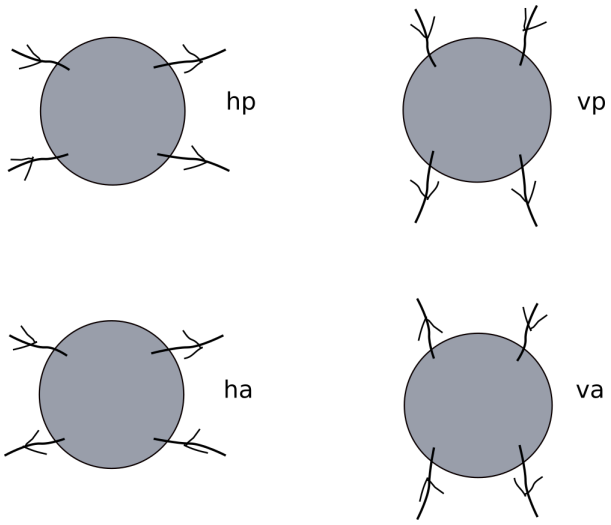

Figure 5.1: The 4 possible cases based on Seifert decomposition parities.

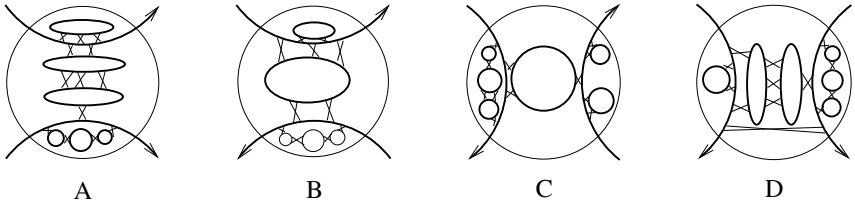

Figure 5.2: The possible scenarios after smoothing all crossings in the tangle T in each case.

the horizontal centerline of T . At the Seifert graph level, the subgraph G_1 of $G_S(D_1)$ corresponding to the Seifert circles contained in T is connected to the rest of graph through the vertices v_1, v_2 corresponding to C_1 and C_2. In other words, v_1 and v_2 form a two- cut for G_1, and the subgraph G_2 of $G_S(D_2)$ corresponding to the Seifert circles contained in T is obtained from G_1 by a Type A Whitney flip using v_1, v_2 as the two-cut and the edge corresponding to the crossing O.

Case B: A flype moves the crossing O between both C_1 and C_2 before and after the flype. At the Seifert graph level, the sub- graph G_1 of $G_S(D_1)$ corresponding to the Seifert circles contained in T is a union of blocks with v_1 being their defining cut vertex. $G_S(D_2)$ is obtained from $G_S(D_1)$ by performing a Type B Whitney flip on G_1 around e.

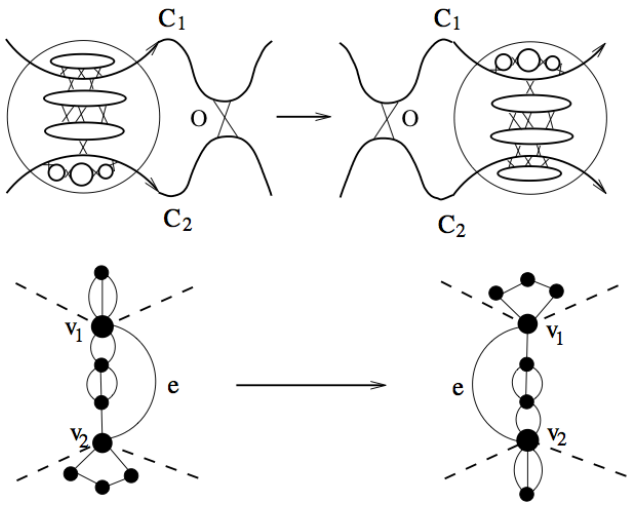

Figure 5.3: Top: the effect of a flype move on a tangle T and crossing O in the case of Seifert decomposition parity hp, which is relabelled to Type A. Bottom: the corresponding actions on $G_S(T)$, which corresponds to Whitney flip Type A in Definition 1.2.16.

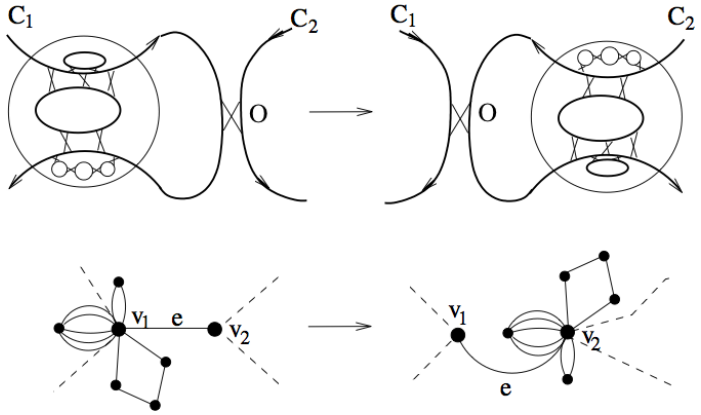

Figure 5.4: Top: the effect of a flype move on a tangle T and crossing O in the case of Seifert decomposition parity ha, which is relabelled to Type B. Bottom: the corresponding actions on $G_S(T)$, which corresponds to Whitney flip Type B in Definition 1.2.17.

Case C: The crossing O is a single crossing between the Seifert circle C_0 and C_2 in the diagram D_1, and becomes a single crossing between C_0 and C_1 in the diagram D_2. At the Seifert graph level, the subgraph G_1 of $G_S(D_1)$ corresponding to the Seifert circles contained in T is $v1$-dependent in $G_S(D_1)$ e where e is the unique edge between v_0 and v_2 corresponding to O.

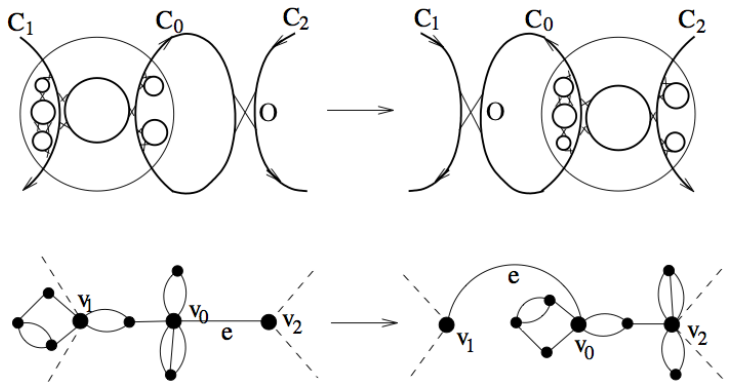

Figure 5.5: Top: the effect of a flype move on a tangle T and crossing O in the case of Seifert decomposition parity va, which is relabelled to Type C. Bottom: the corresponding actions on $G_S(T)$, which corresponds to Whitney flip Type C in Definition 1.2.18.

Case D: There are two sub-cases for Case D.

Sub-case D1: Figure 5.6 illustrates how $S(D_1)$, $S(D_2)$ are related by the flype at T and O, where the s-circles C_1 and C_2 are distinct from each other, and the crossing O is a single crossing between the Seifert circle C_0 and C_2 as shown in Fig. 13 in D_1, and becomes a single crossing between C_0 and C_1 in D_2. At the Seifert graph level, the subgraph G_1 of $G_S(D_1)$ corresponding to the Seifert circles contained in T is $v1$-dependent in $G_S(D_1)$ e where e is the single edge between v_0 and v_2 corresponding to O. This is in fact, a Whitney flip Type C as defined in Definition 1.2.18.

Sub-case D2: We have $C1 = C2$, as illustrated in Figure 5.7. In this case, the subgraph G_2 of $G_S(D_1)$ corresponding to the Seifert circles (and the crossings among them) contained in T as well as the crossing O is $v1$-dependent and $G_S(D_2)$ is obtained from $G_S(D_1)$ by performing a Type D Whitney flip as in Definition 1.2.19, which is a special case of Type A Whitney flip as defined in Definition 1.2.16. Notice that this is special since v_0 is not connected to v_1 by any path not going through G_2, while this is allowed in the definition of a Type A Whitney flip.

We note that in the above analysis, Whitney flip moves change only the local structure involved in $S(D_1)$. Within each block, the edge set and edge weights remain

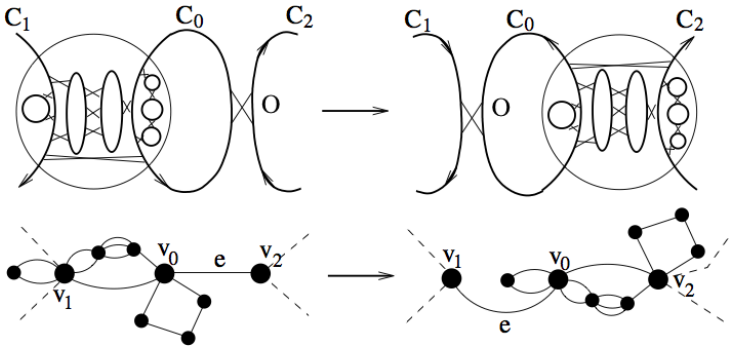

Figure 5.6: Top: the effect of a flype move on a tangle T and crossing O in the case of Seifert decomposition parity vp, which is relabelled to Type D, where the s-circles C_1 and C_2 are distinct from each other. Bottom: the corresponding actions on $G_S(T)$, which corresponds to Whitney flip Type C in Definition 1.2.18.

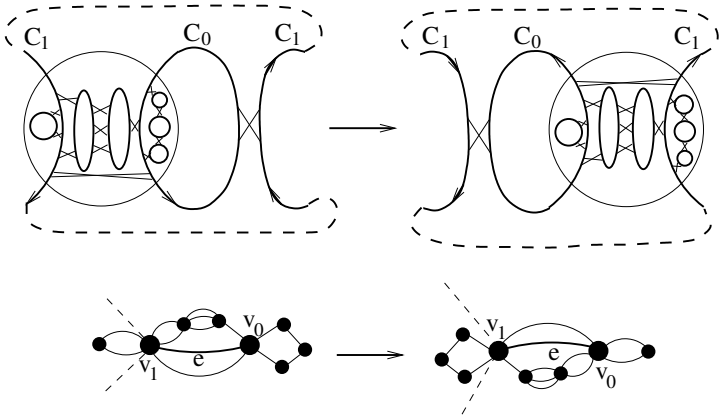

Figure 5.7: Top: the effect of a flype move on a tangle T and crossing O in the case of Seifert decomposition parity vp, which is relabelled to Type D, where $C1 = C2$. Bottom: the corresponding actions on $G_S(T)$, which corresponds to Whitney flip Type A in Definition 1.2.16.

unchanged by a Whitney flip. In section 5.5, we will illustrate how these Whitney flip moves position themselves in the global structures of the Seifert graph of a link diagram.

5.2 Flip Equivalence Classes

Since we have established a relationship between flypes in a reduced alternating link diagram D with Whitney flip moves in the Seifert graph $G_S(D)$, we have set up the ground to identifies quantities in $G_S(D)$ that are preserved under Whitney

flip moves. The four cases in Section 5.1 prove Theorem 5.2.1, which characterizes the correspondence between alternating links under flypes and their graphs under Whitney flip moves.

Theorem 5.2.1. *If two link diagrams D_1 and D_2 are related by a sequence of flype moves, then their Seifert graphs $G_S(D_1)$ and $G_S(d_2)$ are related by a sequence of Whitney flips of types A, B, or C. We denote this as $G_S(D_1) \stackrel{f}{\equiv} G_S(D_2)$.*

5.3 Definition of Writhe-like Invariants

Definition 5.3.1. *We say that an invariant is a writhe-like invariant if, like the writhe, it is an invariant when restricted to the class of reduced alternating link diagrams.*

In this section, we introduce several quantities as writhe-like invariants, most of which were published in [20].

Definition 5.3.2. Let D be a reduced alternating link diagram that is un-splittable (*i.e.* both $G_S(D)$ and $\tilde{G}_S(D)$ are connected). Let $\{B_1, B_2, ..., B_k\}$ be the set of all blocks in $\tilde{G}_S(D)$.

If D is a reduced alternating link diagram, it is well known that D is homogeneous. That is, the crossings on one side of any Seifert circle are of the same sign, while the crossings on the other side of the Seifert circle are of the opposite sign. It follows that all crossings belonging to the same s-block have the same sign, and s-blocks whose level numbers differ by an odd integer contain crossings of different signs.

(i) $w_+(D)$ and $w_-(D)$: the sum of all positive edge weights and the sum of all negative edge weights in $\tilde{G}_S(D)$ respectively;

(ii) $\xi_+(D)$ and $\xi_-(D)$: the number of positive blocks and the number of negative blocks in $\tilde{G}_S(D)$ respectively, where a block is said to be *positive (negative)* if the

weights in it are of positive (negative) sign;

(iii) $W(D)$: the set of all edge weights in $\tilde{G}_S(D)$;

(iv) $\epsilon(D)$: the number of (simple) edges of $\tilde{G}_S(D)$;

(v) $w_B(D) = \{w(B_1), w(B_2), ..., w(B_k)\}$ where $w(B_j)$ is the sum of weights of edges of B_j;

(vi) $W_B(D) = \{W(B_1), W(B_2), ..., W(B_k)\}$ where $W(B_j)$ is the set of all edge weights in B_j;

(vii) $\beta(D)$: The Betti number $\beta(D)$ of $\tilde{G}_S(D)$, which is defined as $\beta(D) = \epsilon(D) - v(D) + 1$, where $v(D)$ is the number of vertices in $\tilde{G}_S(D)$;

(viii) $\hat{\beta}(D)$: which is defined as the set $\{\beta(B_1), \beta(B_2), ..., \beta(B_k)\}$;

(ix) $\Gamma(D)$: which is defined as the set $\{\gamma(B_1), \gamma(B_2), ..., \gamma(B_k)\}$ where $\gamma(B_j)$ is the length of a longest cycle in a block B_j ($\gamma(B_j) = 0$ if B_j contains no cycles).
(x) $\kappa(D)$: the circumference of $\tilde{G}_S(D)$. If $\tilde{G}_S(D)$ is a tree, then $\kappa(D) = 0$.

Theorem 5.3.3. *Each quantity above is a writhe-like invariant, that is, it is a link invariant within the space of all reduced alternating link diagrams.*

Proof. As shown in Section 5.1, Whitney flips do not change a block, but possibly the position of a weight ± 1 edge within a block. That is, if a block has negative or positive edge weights, they remain so under Whitney flip moves. It follows that the pairs $w_+(D)$ and $w_-(D)$ in (i) and $\xi_+(D)$ and $\xi_-(D)$ in (ii) are writhe-like invariants.

$w_B(D)$, and $W_B(D)$ are writhe-like invariants as a consequence $W(D)$ being invariant.

$\beta(D)$, $\hat{\beta}(D)$ and $\Gamma(D)$ are writhe-like invariants since a Whitney flip cannot change a cycle, except the position of an edge with weight ± 1 in a cycle.

Since $\beta(D)$ is invariant, the set of cycle basis remains unchanged, hence the length of the longest cycle of the graph $\tilde{G}$, or its circumference $\kappa(D)$ is also invariant.

□

We say that an invariant is stronger than another one if it can distinguish all link types the other invariant can, but not vice versa. For example, $w_+(D)$ and $w_-(D)$ together is stronger than $w(D)$; $W(D)$ is stronger than $w_+(D)$ and $w_-(D)$ combined; $w_B(D)$ is stronger than $\xi_+(D)$ and $\xi_-(D)$ combined; $W_B(D)$ is stronger than $w_B(D)$ and also stronger than $W(D)$. Moreover, some of the listed invariants cannot be compared with each other. For example, there are distinct reduced alternating link diagrams that $\beta(D)$ can distinguish, but not $w_B(D)$, and vice versa. In Chapter 6, we will quantify the strength of an invariant in the context of tabulated knot diagrams.

5.4 Coupled Edges

This section describes to what extent WF moves can change the structure of a graph at a cut vertex, as well as what remains invariant, which depends on the diagrammatic features of D. We consider a local structure $L(D)$ that includes two vertices v_1 and v_2 of a Seifert graph $G_S(D)$ of the alternating link diagram D, both attached to a vertex v by edges of different signs. Then v must be a cut vertex of $G_S(D)$. To show the quantities that remain unchanged under flypes, we examine the corresponding Seifert circle decomposition $S(D)$. Let C, C_1, and C_2 be the s-circles corresponding to v, v_1, and v_2. Let $c(C_1)$ and $c(C_2)$ be the sets of crossings between C and C_1, C and C_2 respectively. If we travel along C once, we will encounter each crossing in $c(C_1)$ and $c(C_2)$ exactly once. A set of crossings from $c(C_1)$ ($c(C_2)$) is said to form a *cluster*

if it is a maximal set with the property that we can use one of them as a starting point to travel along C to reach the last crossing in the set without encountering any crossing in $c(C_2)$ ($c(C_1)$). We say that the two simple edges (v, v_1) and (v_1, v_2) are coupled if the total number of clusters is 4 or more. At the Seifert diagram level, the multiple crossings $c(C_1)$ and $c(C_2)$ interlock each other in clusters of different signs. In $G_S(D)$, we break down the total edge weights (v, v_1) and (v_1, v_2) to describe how the edges are coupled. The left side of Figure 5.8 shows (a portion of) a link diagram containing coupled edges with 4 clusters and the right side is an example containing no coupled edges. Let us consider what happens to coupled edges when a WF move

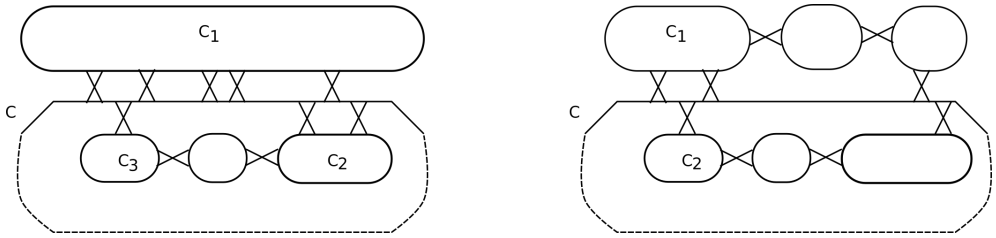

Figure 5.8: Left: a (part of a) Seifert diagram that contains coupled edges with 4 clusters. Right: a (part of a) Seifert diagram that contains no coupled edges.

is applied. We wish to show that a WF move cannot break the couple nor change the number of clusters. We consider how a cluster may be affected by a flype, by considering the configurations of local structure of a flype. Figure 5.9 outlines two sub-cases where the two strands of the tangle T are oriented in the same way, and Figure 5.10 - in opposite ways. The crossing O corresponds to the edge e among multiple edges between v and v_1 in a couple. Consider a minimal couple (one with only 4 clusters). If the rest of edges $(v, v_1) \setminus e$ belong to the flyping structure, without the loss of generality, let the couple structure be $[i_4, i_1, i_2, i_3]$ where e is counted in i_4. Then after the flype, this structure becomes $[i_1, i_2, i_3, i_4]$. We observe that the cyclic order of a couple is preserved. At the Seifert graph level, these two cases would correspond to WF Type A and Type D. In the case of Type A, all crossings between the two Seifert circles are either all within or outside the tangle except that one of

them may be used as the crossing for the flype. If $(v, v_1) \setminus e$ does not belong to the flyped structure, i.e they are outside of the tangle T, then they are not affected by the flype, hence i_4 and the couple structure $[i_4, i_1, i_2, i_3]$ are not affected by the flype. In the case of Type D, we have two sub-cases, one is similar to Type C, which will be considered shortly; the other sub-case is that the couple with v_1 must be within the flype structure and the flype is only a reflection hence we have either $[i_4, i_1, i_2, i_3]$ or $[i_1, i_2, i_3, i_4]$. That is to say, the couple structure is unchanged by a flype.

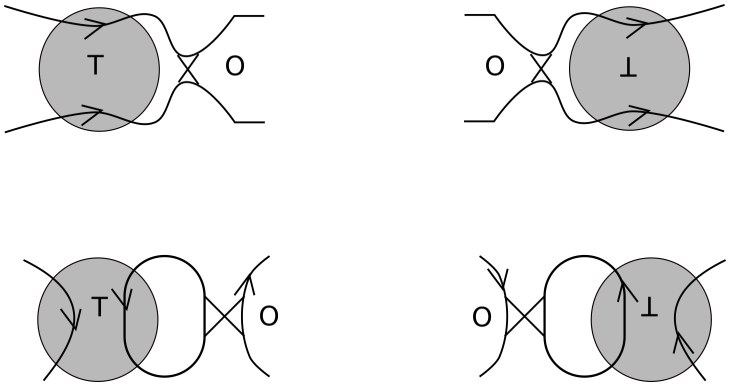

Figure 5.9: The cases when a flype involves parallel tangles.

In the cases that the flyped structures involve antiparallel tangles, as illustrated in Figure 5.10, the corresponding WF moves are of Type B and Type C. In the case of Type B, then all crossings between the two Seifert circles are either all within or outside the tangle except that one of them may be used as the crossing for the flype. If $(v, v_1) \setminus e$ are all outside of the flype structure, which is unaffected by the flyping process, the relative position of e to the tangle T does not change i_4, thus the couple structure $[i_4, i_1, i_2, i_3]$ remains invariant in a flype. If $(v, v_1) \setminus e$ are all inside T, the clusters i_4, i_1, i_2, i_3 are not affected by the flype; only the cyclic order of i_4 is.

In the case of Type C, then the crossing used for the flype cannot be a crossing in the lock since then the number of clusters can only be 2 between C_1 and C_2 if one of them has a single crossing with C_0. In other words, it is not possible for $(v, v_1) \setminus e$ to be a part of the flype structure (i.e. inside the tangle T). So whether i_1, i_2, i_3 are

completely within T or not, the flype only moves e from one side of i_1, i_2, i_3 to the other. So the order of the clusters remains after a Type C move.

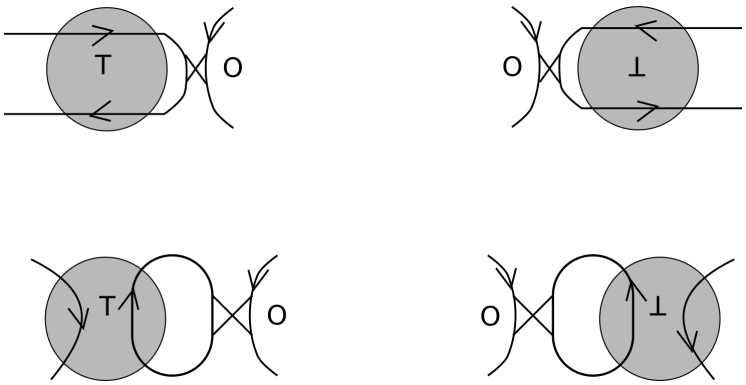

Figure 5.10: The cases when a flype involves antiparallel tangles.

In all cases, we have observed that the number of crossings in each cluster and the cyclic order of these clusters along the Seifert circle C_0 are all preserved.

5.5 Consequences of Whitney Flips on Seifert Graphs of Alternating Link Diagrams

$L(D)$ can belong to one of the following 4 cases:

1. Free edges in a tree.

   Suppose the edge v, v_1 is not coupled with v_1, v_2 in $L(D)$ and the Seifert graph of the whole diagram D, $G_S(D)$ is a tree. v, v_1 must not be a single edge, otherwise the diagram D is nugatory at this crossing. The multigraph $G_S(D)$ admits a type of WF moves if there exists a single edge e among those of v, v_1 to perform a flype in the Seifert decomposition of D. This scenario can happen only with Type A. Figure 5.11 illustrates the single edge e as one of the many edges between v, v_1. On the other hand, if the edges apart from e in v, v_1 can be moved freely, there must be a band between v and v_1, which means there exists a connected sum between these two vertices. This scenario does not happen in a prime link.

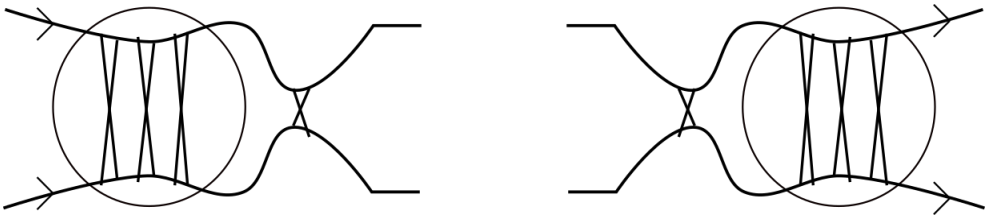

Figure 5.11: Flype one of the multi-edges.

2. Coupled edges in a tree.

   This scenario can happen only with Type A. Since the flype involves all crossings between two separate Seifert circles, the orientation of the tangle must be parallel and the tangle must be of type 0.

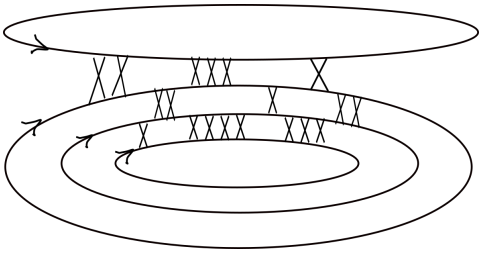

Figure 5.12: Coupled edges cannot be broken in a tree.

   Figure 5.13 shows an example in which the Seifert graph $G_S(D_1)$ is a tree that has 2 pairs of interlocked edges (2 couples), and $G_S(D_2)$ is a tree with a block that can be moved freely along any other vertices by a Whitney flip move. So in $G_S(D_1)$, there exists none of the Whitney flip moves can break the structure $\Phi = \{[1, -2, 6, -3], [2, -2, 5, -3]\}$.

3. Free beads in a cycle. In this case, the free bead need not form a connected sum with the cycle. Figure 5.14 shows an example, where the free bead is the block with 2 multi-edges. The coupled edges are between v_4 and one of the three vertices v_1, v_2, v_3. As a result, in this example the free bead seems to move "freely" among the vertices of the cycle that it is coupled with.

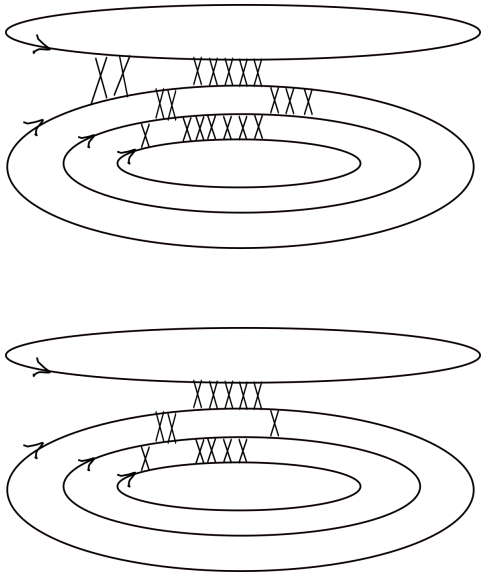

Figure 5.13: Seifert decompositions of D_1 (top) and of D_2 (bottom)

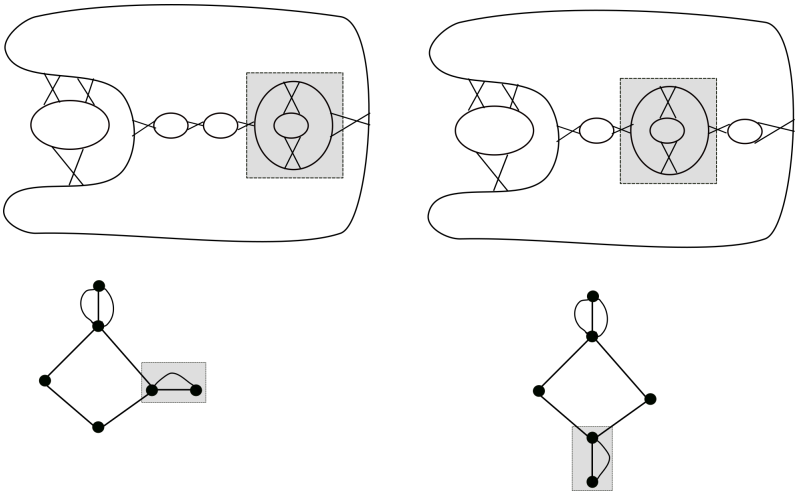

Figure 5.14: A free bead that can move along a cycle by WF moves.

4. Coupled edges in a cycle.

   Whether in the global structure, the diagram contains a cycle or not, we have shown that Whitney flip moves involve a change only on a local (visible) part of the diagram, as shown in Section 5.1. The cyclic order of the crossings in a couple is not affected by Whitney flip moves of any type.

   Based on the observations above, we have the following theorem.

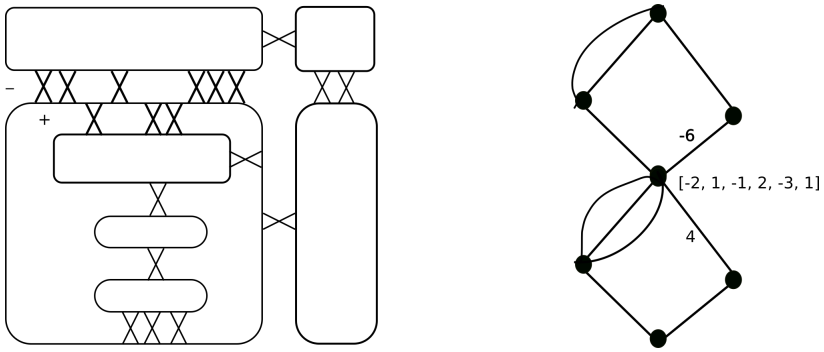

Figure 5.15: Left: A Seifert diagram with a cycle that contains coupled edges. Right: the edges -6 and 4 forms a couple $\Phi = [-2, 1, -1, 2, -3, 1]$.

Theorem 5.5.1. *Let $\Phi(D) = \{\vec{\phi}_1, \vec{\phi}_2, ..., \vec{\phi}_m\}$, where m is the total number of coupled edges and $\vec{\phi}_j$ is a vector consisting of the number of clusters in the j-th couple according to their cyclic order along the orientation of the Seifert circle of the cut vertex v, then $\Phi(D)$ is a writhe-like invariant.*

The 4 cases above also discuss what cannot be changed (1) and what can be changed (2) by Whitney flip moves in a Seifert graph of an alternating diagram D, when a couple structure is involved, whether D contains a connected sum or not. $\Phi(D)$ is an example for case (1).

CHAPTER 6: APPLICATIONS

6.1 The Strength of Writhe-like Invariants

In the study of link invariants, we are in a search for invariants that can distinguish as many links from one another as possible. We are yet to find the ideal invariant that yields a distinct value for each link type. Even though writhe-like invariants are invariant only when we restrict ourselves to the class of reduced alternating links, it is relevant to discuss how powerful they are at distinguishing knots, links within the restriction. This section discusses the strength of an invariant of tabulated minimal diagrams, that we call the t-strength in Definition 6.1.1. We will also compare writhe-like invariants with classical link invariants such as genus, braid index, Kauffman polynomial X, and Jones polynomial.

Definition 6.1.1. *Let $\mathbb{I}$ be an invariant of alternating link diagrams. For each given crossing number cr, we can partition the set of all alternating link diagrams with crossing number cr into subsets $c_1, c_2, ..., c_k$ such that two links belong to the same c_j, for $1 \leq j \leq k$, if and only if they share the same $\mathbb{I}$ value. Then we define $\tau(cr, \mathbb{I})$ be the t-strength of the invariant $\mathbb{I}$ as follows:*

$$\tau(cr, \mathbb{I}) = \frac{k}{\sum_{j=1}^{k} |c_j|},$$

where $\sum_{j=1}^{k} |c_j|$ is the total number of alternating link diagrams with crossing cr.

We calculated the quantities $W(D)$ and $\beta(D)$ as described in Definition 5.3.2 for all alternating knot diagrams in the knot tables in the KnotTheory package [21] up to 16 crossings and for alternating links up to 11 crossings. Tables 6.1 and 6.3 show

a few examples for alternating knot diagrams of 12 crossings.

Table 6.1: A few values of $W(D)$ for alternating knots of 12 crossings and the corresponding number of diagrams sharing the same value of $W(D)$.

$W(D)$	Number of diagrams sharing the same $w(D)$
{4, -5, 1, 1, 1}	1
{3, 2, -3, 4}	2
{3, -2, 5, -2}	3
{6, -6}	19

We can interpret Table 6.1 as follows: There is only one tabulated 12-crossing alternating knot diagram D with the value $W(D) = \{4, -5, 1, 1, 1\}$. There are 2 diagrams D_1, D_2 with the value $W(D_1) = W(D_2) = \{3, 2, -3, 4\}$, 3 diagrams that yield the edge weight set of $\{3, -2, 5, -2\}$, and 19 diagrams that yield the edge weight set of $\{6, -6\}$.

Table 6.2 shows the number of appearances of all values of c_j of all minimal alternating 12-crossing knot diagrams. We use Table 6.2 to calculate $\tau(12, W(D))$.

Table 6.2: Number of alternating knot diagrams of 12 crossings sharing c_j values of $W(D)$.

c_j	Number of diagrams sharing c_j values of $W(D)$
1	343
2	120
3	47
4	19
5	13
6	14
7	6
8	7
9	8
10	4
11	1
12	3
19	1
20	1
21	1
22	1

Table 6.3: Number of alternating knot diagrams of 12 crossings sharing the same values of $\beta(D)$.

$\beta(D)$	Number of diagrams sharing the same $\beta(D)$
0	421
1	462
2	296
3	92
4	17

Similarly, Table 6.3 implies that there are 421 alternating 12-crossing knot diagrams D whose $\beta(D) = 0$, while only 17 diagrams D' with $\beta(D') = 4$.

To compare the t-strength of edge weight set $W(D)$ and Betti number $\beta(D)$ with a classical invariant, we counted the number of tabulated 12-crossing knot diagrams which share the exact same genus $g(D)$. The first row of Table 6.4 can be interpreted as there are 3 knot diagrams whose genus is 1 among the 12-crossing knot diagrams.

Table 6.4: Number of alternating knot diagrams of 12 crossings sharing the same genus.

$g(K)$	Number of diagrams sharing the same $g(K)$
1	3
2	71
3	78
4	495
5	641

We now have the following t-strength values for each aforementioned quantities, in

order to state that $W(D)$ is relatively stronger than $g(D)$ and $\beta(D)$.

$$\tau(12, W(D)) = \frac{343+120+47+19+13+14+6+7+8+4+1+3+1+1+1+1}{1288}$$
$$= 0.457298;$$

$$\tau(12, g(K)) = \frac{1+1+1+1+1}{1288} = 0.00388199;$$

$$\tau(12, \beta(D)) = \frac{1+1+1+1+1}{1288} = 0.00388199$$

$$\implies \tau(12, \beta(D)) = \tau(12, g(K)) < \tau(12, W(D)).$$

The t-strength of $W(D)$ for 11-crossing alternating links is computed based on Table 6.5 as follows:

$$\tau_{link}(11, W(D)) = \frac{211+59+14+10+5+4+4+3+1+1+1}{548} = 0.571168.$$

Table 6.5: Number of alternating link diagrams of 11 crossings sharing the same $W(D)$.

c_j	Number of diagrams sharing the same $W(D)$
1	211
2	59
3	14
4	10
5	5
6	4
7	4
8	3
9	1
12	1
15	1

Table 6.6 gives an idea of where $\tau(12, \beta(D))$ and $\tau(12, W(D))$ are in comparing with the t-strength of genus $g(K)$, braid index $br(K)$, Kauffman polynomial X $f(L))$ and Jones polynomial $V_K(t)$.

Table 6.6: The *t-strength* of $\beta(D)$ is about the same as one of invariants defined over all possible configurations. The *t-strength* of $W(D)$ is in the middle of the comparison spectrum.

Crossing number	$\tau(cr, g(K))$	$\tau(cr, br(K))$	$\tau(cr, W(D))$	$\tau(cr, f(D))$	$\tau(cr, V_K(t))$
9	0.097561	0.097561	0.878049	1	1
10	0.0325203	0.0325203	0.747967	0.95935	0.934959
11	0.00388199	0.00388199	0.553134	0.893733	0.893733
12	0.00388199	0.00388199	0.457298	0.810559	0.832298

6.2 Some Relationships of Writhe-like Invariants to General Invariants

The following observations illustrate that some invariants from Definition 5.3.2 can be informative by relating to other (general) invariants.

Remark 6.2.1. For a reduced alternating link diagram D of a knot K, if $\tilde{G}_S(D)$ is not a tree, then $g(K) \geq \frac{c(D)-\epsilon(D)+1}{2}$, where $c(D)$ is the number of crossings of D and $\epsilon(D)$ is the number of simple edges in $\tilde{G}_S(D)$.

$\tilde{G}_S(D)$ is not a tree implies that $\beta(D) = \epsilon(D) - s(D) + 1 \geq 1$. Then, we have $s(D) \leq \epsilon(D)$. We apply Proposition 4.1.1 to get the desired inequality.

Corollary 6.2.2. *For a reduced alternating diagram D of a knot K with at least 5 crossings, if $\beta(D) = 0$, then $g(K) \geq 2$.*

We have $\epsilon(D) = s(D)$ for $\beta(D) = 0$. So $\epsilon(D) \geq 2$. From $g(K) \geq \frac{c(D)-\epsilon(D)+1}{2}$, we have $g(K) \geq \frac{5-2+1}{2} = 2$.

Remark 6.2.3. Let D be a homogeneous link diagram, if $\tilde{G}_S(D)$ is Hamiltonian, then D is positive.

If $\tilde{G}_S(D)$ is Hamiltonian, then $\tilde{G}$ must not contain any cut vertex. Suppose the contrary, i.e. $\tilde{G}$ contains a cut vertex w, let v be the start of a Hamiltonian cycle in $\tilde{G}_S(D)$ such that $v \neq w$. Then one traversing this Hamiltonian cycle must have passed both w and v twice, contradicting the definition of a Hamiltonian cycle in Definition 1.2.8. On the other hand, D is homogeneous, which implies that $\tilde{G}_S(D)$ is homogenous. So $\tilde{G}$ is one block where the sign of the edges are all the same, hence the result follows.

It is important to note that Hamiltonian property of $\tilde{G}_S(D)$ leaves out many positive links. Since an s-graph is bipartite, the number of vertices of $\tilde{G}_S(D)$ must be even by Proposition 1.2.13, and by Remark 4.2.10, if D is a knot diagram, then we

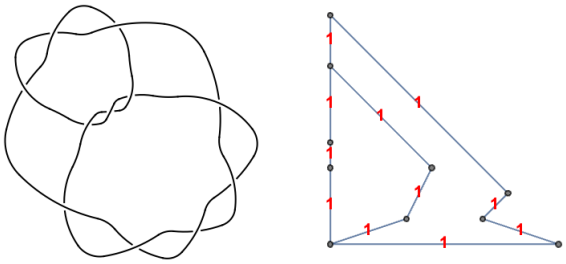

Figure 6.1: The knot $11a_{362}$ and its s-graph.

are referring to only positive diagrams with odd number of crossings in Remark 6.2.3. Figure 6.1 shows a non-Hamiltonian s-graph of a positive knot with 11 crossings.

Writhe-like invariants can be used in combination with other invariants to distinguish links. Though $\tau(12, W(D)) < \tau(12, f(D) < \tau(12, V_K(t))$, there are multiple 12-crossings knots that have the same Kauffman X or Jones polynomial, and different writhe-like invariants. The computation of $\tau(12, V_L(t))$ is based on the data in Table 6.7.

Table 6.7: The number of alternating knot diagrams of 12 crossings sharing j Jones polynomials.

The value j	Number of diagrams sharing j values of $W(D)$
1	907
2	128
3	26
4	8
5	3

Example 6.2.4. *However, there exist knots which share the same genus, Kauffman X, and Jones polynomials. Figure 6.2 is an example of such case:*

$$\nabla_{12_{a598}}(z) = f_{12_{a954}}(z) = A^{36} - 4A^{32} + 9A^{28} - 17A^{24} + 25A^{20} - 31A^{16} + 34A^{12} + \frac{1}{A^{12}} - 31A^{8} - \frac{4}{A^{8}}$$

$$V_{12_{a598}}(t) = V_{12_{a954}}(t)$$

$$= t^{-3} - 4t^{-2} + 10t^{-1} - 18 + 26t - 31t^2 + 34t^3 - 31t^4 + 25t^5 - 17t^6 + 9t^7 - 4t^8 + t^9.$$

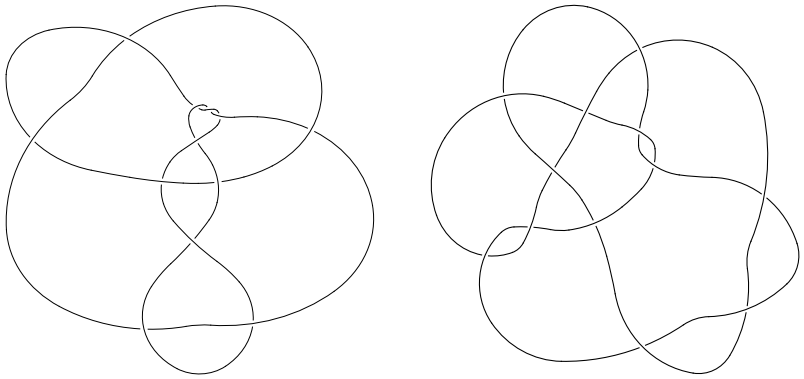

Figure 6.2: Left: a minimal diagram D_1 of the knot 12_{a598} with $W(D) = \{1, 2, 2, 3, -4\}$.
Right: a minimal diagram D_2 of the knot 12_{a954} with $W(D_2) = \{2, -4, 4, 1, 1\}$. These knots 12_{a598} and 12_{a954} have the same Kauffman X and Jones polynomial.

Example 6.2.5. In this example, we illustrate that coupled edges can distinguish alternating links with arbitrarily large number of crossings. This is when calculating knot polynomials becomes expensive. Figure 6.3 shows the Seifert circle decompositions $S(D_1)$ and $S(D_2)$ of two 21-crossing alternating knot diagrams D_1 and D_2. The Seifert graphs $\tilde{G}_S(D_1)$ and $\tilde{G}_S(D_2)$ are both simple paths consisting of 3 consecutive edges of weights $\{6, -6, 9\}$. However, the coupled edges have different structures:

$$\Phi(D_1) = \{[2, -1, 3, -2, 1, -3], [2, -1, 3, -2, 4, -3]\},$$

$$\Phi(D_2) = \{[2, -2, 3, -1, 1, -3], [1, -2, 5, -1, 3, -3]\}.$$

So we cannot break the couple structure to perform a cyclic order permutation of Φ. Thus D_1 and D_2 are of different knots.

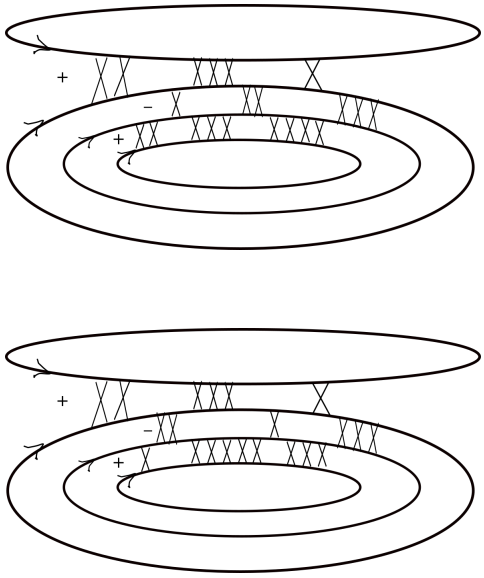

Figure 6.3: The Seifert decomposition of the knot diagram D_1 (Top), and the Seifert decomposition of the knot diagram D_2 (Bottom).

6.3 Completion of Classification of Strongly Invertible Links

Our next example is the proof of a theorem that contains a new result concerning oriented rational links. Thus we need some preparations before we can state and prove the theorem. We shall assume that our readers have some basic knowledge about rational links. [1] is a good reference for readers who are not familiar with the subject. Let p and q be two positive integers with $\gcd(\mathrm{p},\mathrm{q}) = 1$ and $0 < p < q$. Let $(a_1, a_2, ..., a_{2k+1})$ be the (unique) vector of odd length with positive integer entries such that

$$\frac{p}{q} = \frac{1}{a_1 + \frac{1}{a_2 + \frac{1}{\cdots \frac{1}{a_{2k} + \frac{1}{a_{2k+1}}}}}}.$$

For the sake of convenience we will write the above as $p/q = [a_1, a_2, ..., a_{2k+1}]$. It is known that any rational link has a reduced alternating diagram called a 4-plat corresponding to the odd length continued fraction decomposition vector of some positive integers with $\gcd(\mathrm{p},\mathrm{q}) = 1$ and $0 < p < q$ as shown in the Figure 6.4 for the case of $p/q = 278/641 = [2, 3, 3, 1, 2, 3, 2]$. We will write this rational link as $L(p/q)$.

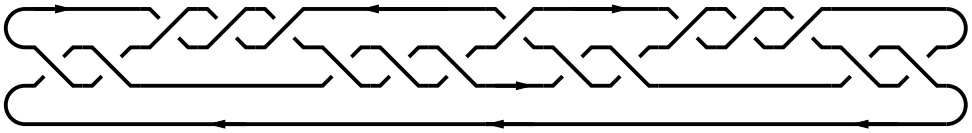

Figure 6.4: The reduced alternating diagram D of the rational knot corresponding to the rational number 278/641 which has the continued fraction decomposition vector $[2, 3, 3, 1, 2, 3, 2]$.

It is known that rational links are invertible, that is, changing the orientations of all components in a rational link will not change the link type. However, in the case that an oriented rational link L has two components (this happens if and only if q is even if L is represented by a 4-plat corresponding to $p/q = [a_1, a_2, ..., a_{2k+1}]$), changing the orientation of only one component of L may result in a rational link that is topologically different from L (as oriented links). L is said to be *strongly invertible* if changing the orientation of one of its component does not change its link type. [22, Theorem 8.1] states that if a two-component rational link $L(p/q)$ is strongly invertible, then $p/q = [a_1, a_2, ..., a_k, \alpha, a_k, ..., a_2, a_1]$ for some integers $a_1 > 0$, ..., $a_k > 0$, $\alpha > 0$. The following theorem strengthens this result.

Theorem 6.3.1. *Let $L(p/q)$ be a two-component oriented rational link (so that* $\gcd(\mathrm{p}, \mathrm{q}) = 1$, $0 < p < q$ *and q is even). Then $L(p/q)$ is strongly invertible if and only if $p/q = [a_1, a_2, ..., a_n, \alpha, a_n, ..., a_2, a_1]$ where $a_1, a_2, ..., a_n$ are positive integers and $\alpha > 0$ is odd.*

Proof. Without loss of generality, the bottom long arc of $L(p/q)$ in its 4-plat form as shown in the top of Figure 6.4. Let $L_1(p/q)$ and $L_2(p/q)$ denote the two rational links by assigning the second component different orientation so that the first crossing from the left is positive in $L_1(p/q)$ and negative in $L_2(p/q)$.

Let us first examine the case when $L(p/q)$ (with q even) is strongly invertible, that is, $L_1(p/q) \sim L_2(p/q)$ and $L(p/q)$ is either $L_1(p/q)$ or $L_2(p/q)$. By [22, Theorem

8.1], $p/q = [a_1, a_2, ..., a_k, \alpha, a_k, ..., a_2, a_1]$ for some integers $a_1 > 0$, ..., $a_k > 0$, $\alpha > 0$. We claim that in this case the right most crossing is negative (positive) in $L_1(p/q)$ ($L_2(p/q)$). If this is not true, say that the right most crossing in $L_1(p/q)$ is also positive, then as we travel along the s-circle containing the long arc starting from the left most crossing, the first and last blocks of $L_1(p/q)$ we encounter are both positive, which implies that $\xi_+(L_1(p/q)) = \xi_-(L_1(p/q))+1$. On the other hand, for $L_2(p/q)$ the first block we encounter is negative, which implies that $\xi_-(L_2(p/q)) \geq \xi_+(L_1(p/q))$, which is a contradiction. This implies that the strands at the left and right ends of the 4-plat $L_1(p/q)$ are as shown in Figure 6.5, in which the middle points marked by 1, 2, 3 and $1'$, $2'$, $3'$ are the points to be connected to create the middle section of $L_1(p/q)$ corresponding to the α crossings. If we start at the point marked by 3 from the left and travel according to the orientation of the strand, we will end at one of the points marked by 1, 2 or 3 in the middle. Let us say we stop at 3 (the other cases can be similarly discussed and are left to the reader). Then since the continued fraction decomposition vector of p/q is a palindrome, if we start at the point marked by $3'$ from the right and travel according to the orientation of the strand, we will also end at the point marked by $3'$ in the middle. If we continue, we will now have to go through the crossings in the middle, since otherwise we will have to connect 3 to $3'$ by a straight line segment but that will violate the orientations. For the same reason, α has to be odd since otherwise we will still have to connect 3 to $3'$ by a strand. Hence the only possibility is that α is odd and the point 3 is connected to the point $2'$ by going through these crossings.

Now, let us consider the case when $p/q = [a_1, a_2, ..., a_n, \alpha, a_n, ..., a_2, a_1]$ where $a_1, a_2, ..., a_n$ are positive integers and $\alpha > 0$ is odd, and q is even (so $L(p/q)$ has two components). Similar to the discussion above, let us consider the partial 4-plat of $L_1(p/q)$ as shown in Figure 6.6. Notice in this case we do not know the orientation of the strand at the right end of the 4-plat that does not belong to the bottom long

strand.

If we start at the point marked by 3 from the left and travel according to the orientation of the strand, then again we will end at one of the points marked by 1, 2 or 3 in the middle. Let us say we stop at 3. 3 cannot be connected to $3'$ by going through the crossings in the middle since α is odd. So if 3 is connected to $3'$ then it is by a straight line segment and the middle crossings will be between points 1, 2 and $1'$, $2'$ in the middle. Since the link has two components, it is necessary that 2 be connected to $2'$ and 1 be connected to $1'$. This is impossible since α is odd. Thus 3 can only be connected to $2'$ by going through the α crossings in the middle, and we shall travel to $1'$ to the right side in order for the link to have two components. This then determines the orientation of the strand at the right side (that does not belong to the bottom long strand), which is the same as that of Figure 6.5. If we now take a 180° rotation of the 4-plat around the y-axis, then we obtain $L_2(p/q)$ (it uses the same vector $[a_1, a_2, ..., a_n, \alpha, a_n, ..., a_2, a_1]$ and starts with a negative crossing on the left).

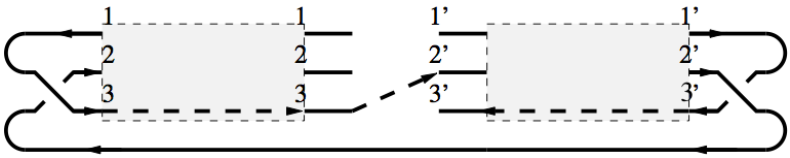

Figure 6.5: The orientations of the strands at the ends of a strongly invertible rational link in the 4-plat form.

There are two cases left. If we start at 3 and end at 1 in the middle, then the discussion is identical to the above. If we start at 3 and end at 2 in the middle, then we have to go through the middle crossings to reach either $1'$ or $3'$ as shown in the bottom of Figure 6.6 for one of the two cases. The remaining argument is similar to the above. □

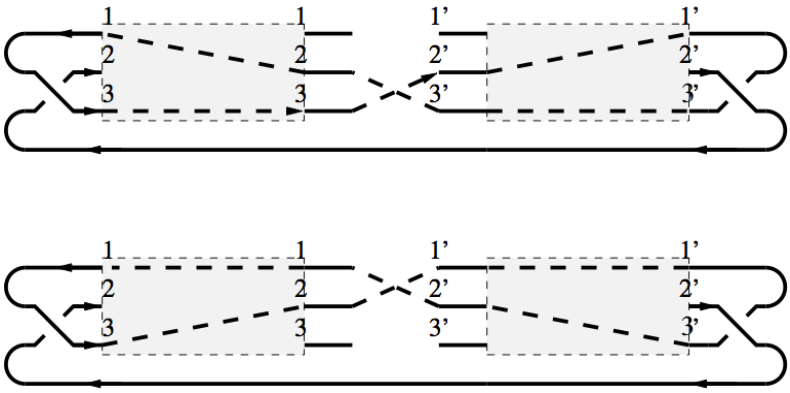

Figure 6.6: Two strands connect with symmetry in the 4-plat form of a rational link.

CHAPTER 7: COMPUTATION OF WRITHE-LIKE INVARIANTS

7.1 Computational Complexity Theory Basics

This section gives an elementary introduction to the studies of how much of a resource, time, a problem can take up. We assume some background in propositional logic. Interested readers may learn more about complexity theory in [23] and algorithm analysis in [24].

Let the function to be estimated be $f(n)$ where n is the number of crossings in a reduced alternating link diagram. Then, by *f(n)=O(g(n))*, we mean $f(n) \leq c.g(n)$ for any constant c and large enough n, i.e. $n \geq N$, for some constant N. We also say that the function $f(n)$ has worst case complexity of $O(g(n))$.

Definition 7.1.1. A *polynomial-time* algorithm is an algorithm that has worst case complexity of $O(n^k)$ for some constant k.

We call a problem *tractable* if and only if there exists a polynomial-time algorithm that solves the problem entirely, and *intractable* if and only if there is not a known polynomial-time algorithm to solve the problem entirely. A problem P_1 is said to *reduce* to problem P_2 if solving P_2 in polynomial-time implies solving P_1 in polynomial-time as well.

A *decision* problem is a problem to which the solution is binary, that is, it takes true or false as the answer.

The set *Non-deterministic polynomial-time (NP)* is defined as the set of all decision problems of which any suggested solution to an instance of the problem can be validated with polynomial-time. We say that a problem is in P if it is in NP and is tractable.

Definition 7.1.2. A problem is *NP-complete* if it is in NP, and every problem in NP reduces to it in polynomial time. A problem is in *NP-hard* if an NP-complete problem reduces to it.

Example 7.1.3 below defines a few more terms in order to state a problem and its complexity class.

Example 7.1.3. *A boolean literal* b, or literal b for short, is an object that must take the value of true or false. The negation of b is often denoted $\bar{b}$, and is considered distinct from b. A *clause* is a finite set of distinct literals joined by only the logical operator "or". A conjunctive normal form (CNF) formula is a finite set of clauses which are joined by the logical operator "and". These concepts allow us to define a *2-Satisfiability (2-SAT)* problem, that is the problem to find an assignment of truth values that leads to the evaluation of a given CNF formula to be true, when every clause has at most 2 literals. 2-SAT is a special case of SAT problems in which clauses can have finite number of literals. The problem SAT is in NP-complete [23].

The problem of deciding whether a given graph is Hamiltonian is another example of an NP-complete problem [23].

When an expected answer for a problem is neither "Yes" or "No", the complexity classes above do not suffice to characterize its complexity. A class of problems that relates to our interest is the class of *counting* problems. For example, instead of asking whether a boolean formula has a satisfiable assignment, we can ask to find the number of distinct satisfiable assignments.

Definition 7.1.4. A problem is said to be in $\#P$ if it is a counting problem and is in NP. A problem is *$\#P$-hard* if every other problem in P has a polynomial time counting reduction to it.

A problem that is #P-hard is at least as hard as an NP-hard problem. Now we are ready to state the well-known results about computation complexity of Jones

and Kauffman polynomials: the computational complexity of Jones polynomial is #P-hard [25] and of Kauffman polynomials is NP-hard [26].

7.2 Computation of Seifert Graphs of a Link Diagram

This section describes the algorithm used to draw the Seifert graph of a link diagram from its Planar diagram codes (Definition 1.1.7). We use the following codes to illustrate our algorithm: *[4, 2, 5, 1], [6, 3, 7, 4], [8, 6, 1, 5], [2, 7, 3, 8]*, which is a PD code of the knot 4_1.

- *DetectSCircles*: browse each tuple to find repeating numbered arcs which form a cycle. From Remark 1.1.8, we search in $n-1$ tuples apart from the first tuple to record the arcs that join together to form an s-circle. As an example, we find 4 which pairs with 6 in the second tuple, and 2 which pairs with 8 in the last tuple. So the first s-circle is formed by the following arcs: *{4, 2, 8, 6}*. The output of this step is a 2-dimensional list which contains the collection of s-circles formed by numbered arcs. In this example, the list is *{{4, 2, 8, 6}, {5, 1}, {3, 7}}*.

- *SeifertAdjacencyMatrix*: We consider each s-circle found in function *DetectSCircles* a vertex, and record a square $n \times n$ matrix. If there are repeating numbered arcs between any two tuples in the previous function, then there exists an edge between the vertices that contains these two tuples. Increment the edge count between these two distinct vertices. Since Seifert graphs do not contain loop edges, then entries on the diagonal of the matrix are zeros. In this example, there are 2 edges between {4, 2, 8, 6} and each of the other vertices {5, 1}, and {3, 7}. The output of this step is an $n \times n$ matrix where n is the number of crossings of the link diagram.

- *GetCrossingSign*: while recording the edge weight, check the sign of the crossing, based on Remark 1.1.8. Since we are dealing with alternating links, if crossings

exist between any 2 s-circles, their signs must be the same. We increment the count of positive edges between corresponding vertices if the edge at hand is positive, and increment the negative edge count between corresponding vertices otherwise. From the 4 tuple in the input example, we see that the crossings *[6, 3, 7, 4], [2, 7, 3, 8]* are negative, and the other two crossings are positive. The output of this step is the crossing sign of the crossing in question.

- *SignedSeifertGraph*: mark down the distinct vertices, then for each non-zero value in the adjacency matrix above, draw a single edge. The signed values from the matrix are used to label edges. Choose *"PlanarEmbedding"* as a graph layout in Mathematica, to output the result as a plane graph.

Proposition 7.2.1 analyzes the worst-case complexity of the computation of writhe-like invariants.

Proposition 7.2.1. *The computation of writhe-like invariants, for n-crossing alternating link diagrams, $f(n)$, is of quadratic order of n.*

Since each tuple (crossing) is accessed once to find elements (numbered arcs) that constitute to any s-circle, and between any two s-circles, crossing signs are traced by looking for repeating numbered arcs in each tuple, we have to go into all tuples twice in depth. Thus this yields $f(n) = O(n^2)$ for an $n-$tuple input, that corresponds to an n-crossing link diagram. Other assignments in the algorithm are of lower or the same order and can be ignored in analyzing the worst-case complexity.

7.3 Derivation of the Edge Weight Sets and Betti Number of Simple Seifert Graphs

Edge weight set: $W(D)$ is simply the weights of all edges of $\tilde{G}_S(D)$, in which the signs of each weight is the sign of crossings in the oriented link diagram D. The edge weight sets $W(D)$ is the nonzero values between two distinct vertices in the adjacency matrix from *SeifertAdjacencyMatrix*.

Betti number: The function that calculates $\beta(D)$ relies on Proposition 1.2.12. For a simple weighted s-graph, we find the cycle basis of $\tilde{G}_S(D)$. This is done via a built-in function of Mathematica, *FindFundamentalCycles* that searches for all basis cycles of a given graph. Then $\beta(D)$ is the length of the list of basis cycles of $\tilde{G}_S(D)$.

7.4 Knot Data Storage and Processing

Data of the following invariants were obtained from knotinfo [27] for alternating knots up to 12 crossings:

- Braid index $br(L)$.
- Jones polynomials $V_L(t)$.

Data of genus $g(L)$ were computed for alternating knots up to 16 crossings, from the function *ThreeGenus* of package knottheory [21]. Data of Kauffman polynomial X was recomputed based on function *Kauffman[][a,z]* of *knottheory* package. All data (including $W(D)$ and $\beta(D)$) are stored in an open source SQL database management system (MySQL) and processed using structured query language. For example, all 12-crossing alternating knots are described in the structure in Figure 7.1, and a query to get how many diagrams are sharing the same value of $\beta(D)$ is shown in Figure 7.2.

```
| cr_12 | CREATE TABLE `cr_12` (
  `id` int(11) NOT NULL AUTO_INCREMENT,
  `minLp` decimal(4,0) NOT NULL,
  `maxLp` decimal(4,0) NOT NULL,
  `averageLp` float NOT NULL,
  `spectrum` blob NOT NULL,
  `alternating` tinyint(4) NOT NULL DEFAULT '1' COMMENT '1: alternating\n0: non-alternating',
  `writhe_like_inv` blob,
  `nsc` int(11) DEFAULT NULL,
  `betti` smallint(6) DEFAULT NULL,
  `unknotting` varchar(45) DEFAULT NULL COMMENT 'unknotting number - as of 07/08/2017 based on knotinfo',
  `braid_index` int(11) DEFAULT NULL COMMENT 'from knotinfo- as of July 18, 2017',
  `bridge_index` int(11) DEFAULT NULL COMMENT 'bridge index from knotinfo as of 07192017',
  `three_genus` int(11) DEFAULT NULL COMMENT 'three genus invariant based on knotinfo as of 08/18/2017',
  `alexander` blob,
  `alexconway` blob,
  `signature` int(11) DEFAULT NULL,
  `jones` blob,
  PRIMARY KEY (`id`)
) ENGINE=InnoDB AUTO_INCREMENT=2177 DEFAULT CHARSET=latin1 |
```

Figure 7.1: The structure of data for 12-crossing alternating knots.

```
mysql> select betti, count(id) as c from cr_12 where alternating =1 group by betti order by c;
+-------+-----+
| betti | c   |
+-------+-----+
|     4 |  17 |
|     3 |  92 |
|     2 | 296 |
|     0 | 421 |
|     1 | 462 |
+-------+-----+
5 rows in set (0.01 sec)
```

Figure 7.2: A query to output how many distinct diagrams share the same value of $\beta(D)$, which is called *betti* in the data storage.

7.5 Future Improvements

The step to assign signs to edge weights is currently separated from tracing edges between s-circles. This can be combined with tracing edges to avoid repeating the browsing of every s-circle. The computation of edge weight set can be improved by grouping entries by graph blocks.

CHAPTER 8: OPEN QUESTIONS AND CONCLUSION

8.1 Seifert Graphs under Reidemeister Moves

The restriction to stay within the class of alternating links allows us to pin down what remains intact when flypes are done on the link diagrams, since the Tait Flyping Theorem [17] provides the tool to define equivalence in this family of links. In other words, outside of the class of alternating links, the quantities in Definition 5.3.2 are no longer link invariants.

To develop this invariant to a general link invariant, one needs to consider what R-moves do to Seifert graphs of any link diagram. We can say much about the changes in $G_S(D)$ when R-moves are performed on the link diagram D in all but one case. As explored in Section 8.1.2, the current graph structure does not suffice to keep track of corresponding changes by a special case of R-III moves.

First we examine the translation of R-I and R-II moves on a link diagram D to the multigraph $G_S(D)$ (by an abuse of terms, we say *R-move on a graph* to mean the effect of an R-move on a link diagram D to the Seifert graph of D).

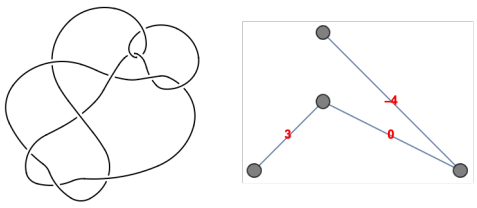

Figure 8.1: An example of an edge weight of 0 in $\tilde{G}_S(D)$ where D is the minimal diagram of the knot $11n_{34}$.

We consider the case when D is non-homogeneous. In the simple edge weighted

Seifert graph of a link diagram, an edge weight should be understood as the total in signs of edges. Figure 8.1 shows an example of an edge weight of 0, which means that the number of positive crossings equals the number of negative crossings between these two respective s-circles in the Seifert decomposition of D.

R-I moves: The consequence of this kind of move on the Seifert graph of a link diagram D is to add or remove a leaf vertex v and a single crossing with v as its end point. On the right of Figure 8.2, a (portion of) vertex u is shown.

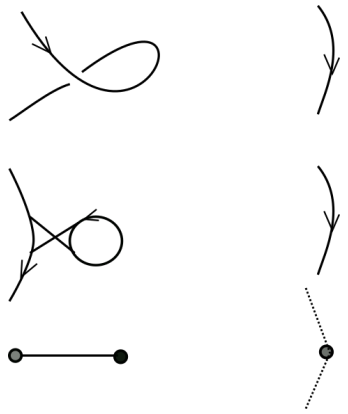

Figure 8.2: Changes in a Seifert graph after Reidemeister move I in a link diagram.

R-II moves: This case has several sub-cases (shown in sub-section 8.1.1), depending on the orientation of the two strands, whether they belong to the same link component, and how they intersect each other. The dashed arcs represent long arcs, which means that intersections with itself or with other components not involved in this Reidemeister move II are not shown.

8.1.1 Sub-cases of Seifert graphs under R-II moves

We use the dash arcs to represent long arcs, where the intersection with itself or with other components not involved in the Reidemeister moves are not shown.

The scenario we consider in sub-case 1 is when the two strands involved in the R-II move belong to two distinct components, as shown on the top of Figure 8.4. The effect of R-II move is recognizable by the appearance of an edge of $+1$ and an edge

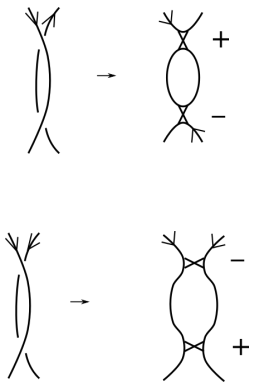

Figure 8.3: The cases given by the orientation of the two strands in Reidemeister move II. Top: Case 1. Bottom: Case 2.

of -1.

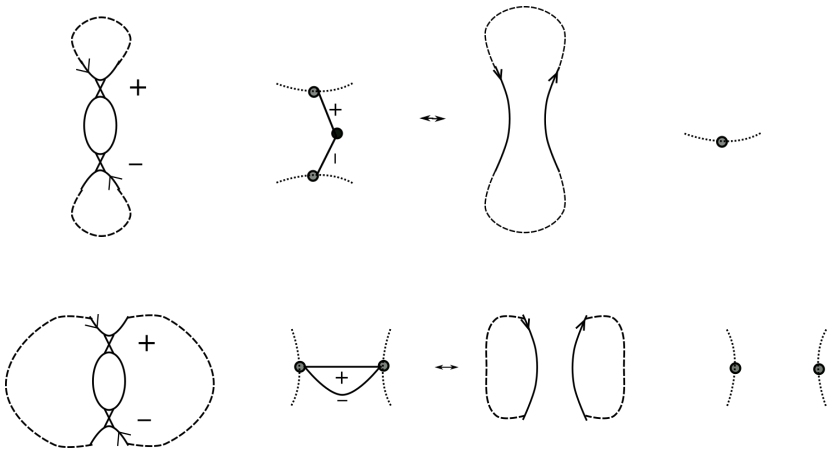

Figure 8.4: The effects on Seifert graphs when an R-II move is performed on a link diagram.

In the sub-case 2, the two strands in R-II move belong to the same s-circle. In the corresponding Seifert graph, we observe 2 loops with opposite signs. Since we do not consider Seifert graphs with loop edges, this case is eliminated.

Figure 8.5 illustrates for sub-cases 3 and 4.

The sub-cases 3 and 4 are similar to sub-cases 1 and 2 respectively, with the difference only in the orientations of the strands, shown in Figure 8.5. In sub-case 3, the move is recognizable if it is an R-move that increases the number of crossings.

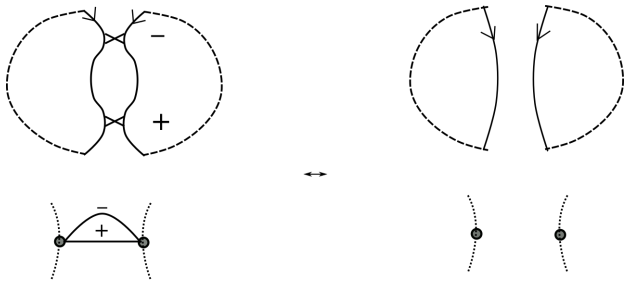

Figure 8.5: We note there can be crossings between these two s-circles and other components not shown in this figure.

In sub-case 4, the two apparently-separated s-circles may have crossings with s-circles in other components, not involved in this R-move, so we do not have a disconnected graph. The bottom of Figure 8.5 shows that the R-move is recognizable by a pair of edges of opposite signs.

Next, we consider how R-III moves affect the Seifert diagram of a link diagram. We observe that the number of crossings and the signs of crossings are preserved under an R-III move. Since each strand can have either direction and there are 3 strands, the total number of combinations in terms of orientation of the strands is 6. These 6 scenarios make up only 2 distinct cases, shown in Figure 8.6, based on the connection of strands form partial (or full) s-circles after smoothing all 3 crossings.

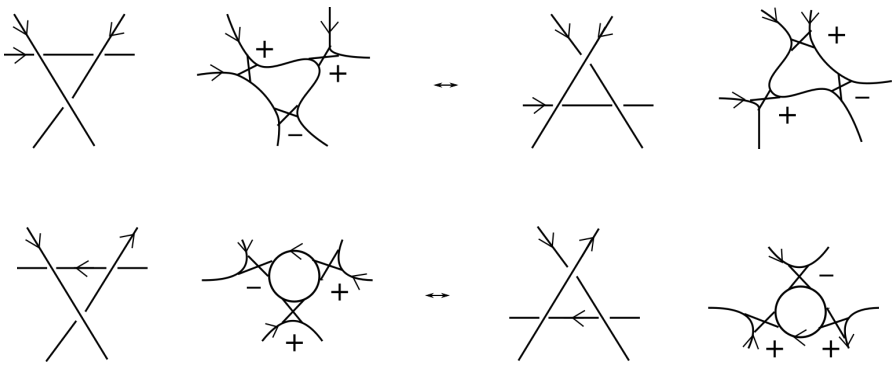

Figure 8.6: The possible orientations of the three strands in an R-III move yield 2 distinct cases (top: case 1, and bottom: case 2). In both cases, the number of crossings and the signs of crossings are preserved under an R-III move.

However, these partial s-circles may connect with each other and the rest of the link diagram in different scenarios, which we will consider in sub-section 8.1.2.

8.1.2 Sub-cases Seifert graph under R-III moves

Since the orientations are arbitrary in considering these sub-cases, we do not mark them on the figures.

Sub-case 1A: In the case shown in Figure 8.7, the three arcs must belong to three distinct s-circles, regardless of the orientations of the three arcs. The signs of edges shown in its corresponding Seifert graphs depend the orientations of the strands. Considering all the possible strand orientation combination, the crossing signs can appear in the following groups: $\{+,+,-\}$, $\{-,-,+\}$, $\{-,-,-\}$, and $\{+,+,+\}$. Since before and after an R-III move, the crossings and their signs are preserved, we will display one group of crossing signs in Figure 8.7.

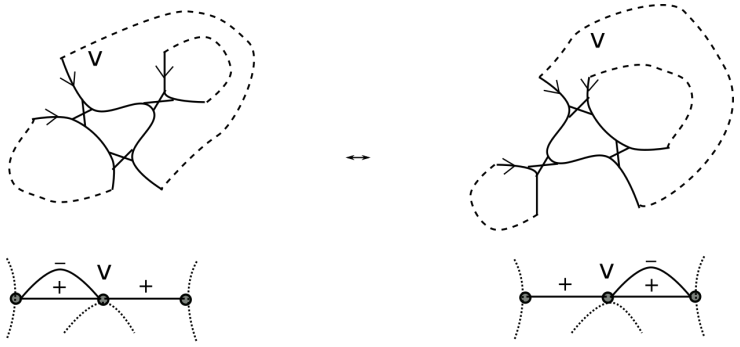

Figure 8.7: Sub-case 1A: The three arcs belong to 3 distinct s-circles, before and after an R-III move. We note that v is necessarily a cut vertex.

In sub-case 1B, the only difference to 1A is the sign of crossings: $\{-,-,+\}$. In sub-case 1C, the crossing signs are $\{-,-,-\}$, and 1D, $\{+,+,+\}$. These cases are not shown on figures.

It turns out that we can trace the change in the Seifert graph when the R-III moves on the diagram D are of cases 1A, 1B, 1C, and 1D.

Next, we consider connection among the three pieces of arc in case 2, shown at the

bottom of Figure 8.6. Sub-cases 2A and 2B are concerned with how these three arcs are connected to each other or to the rest of D.

Sub-case 2A: In Figure 8.8, two out of three arcs join the same s-circle, while the third arc joins a separate s-circle. The Seifert graph of this portion is shown at the bottom of the figure, where we observe that we have the same situation of 3 signed single edges. However, on the right of Figure 8.8, u is necessarily a cut vertex.

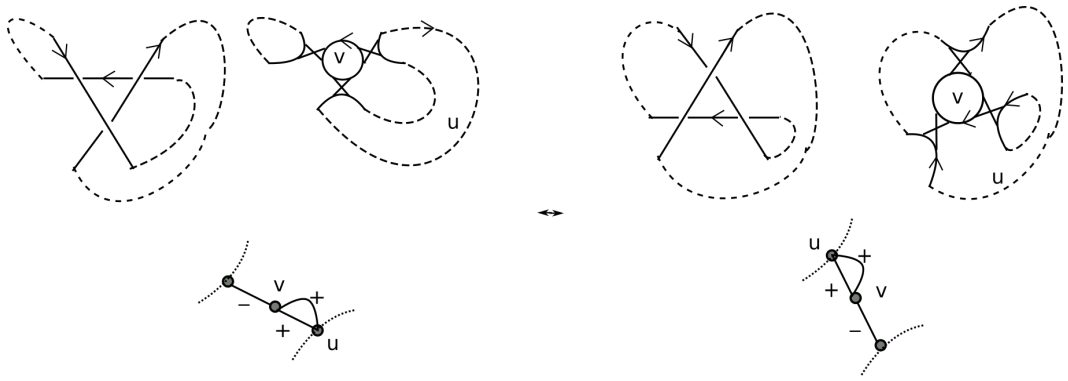

Figure 8.8: Sub-case 2A: An R-III move that keeps the number of vertices and edges unchanged in the visible portion of $G_S(D)$.

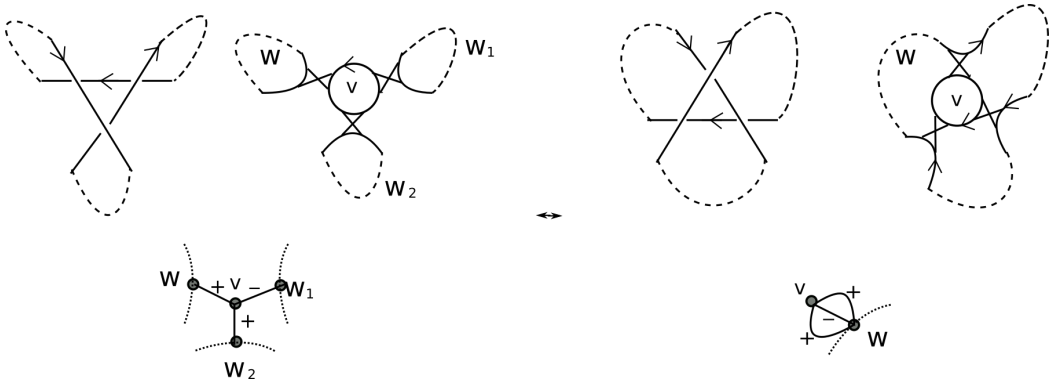

Figure 8.9: Sub-case 2B: An R-III move can change the number of vertices in the visible portion of $G_S(D)$.

Sub-case 2B: The global structure affects the corresponding change in $G_S(D)$ when an R-III move is done on D. In Figure 8.9, we observe that the number of crossings and their signs remain; however, the three arcs which belong to separate s-circles on

the left now join (on the right) to make up a new s-circle. So in $G_S(D)$, as shown on the right of Figure 8.9, vertices w_1 and w_2 are identified with w and the edges (vw_1), (vw_2) are now between v and w. In addition, w is necessarily a cut vertex.

8.2 Conclusion

Writhe-like invariants add up to the toolbox used to distinguish alternating links. Given the polynomial computation time, and the t-strength ranging from 40 to 50% for minimal knot diagrams up to 12 crossings, they can be useful in distinguishing alternating links that index invariants may fall short. They can also be used in addition to a strong invariant like the Jones polynomial, as we have examined that there are links with the same Jones polynomials and different signed edge weight sets.

A natural question would be to generalize the invariants to ambient isotopy. That is, one needs to consider the effects of R-moves on Seifert graphs of a link diagram. From Section 8.1, we observe the following about the number of s-circles $s(D)$ and the number of crossings $c(D)$ in all cases of R-moves: (a) both $s(D)$ and $c(D)$ do not change, or (b) only $s(D)$ changes by ± 2, or (c) only $c(D)$ changes by ± 2, or (d) both $s(D)$ and $c(D)$ change by ± 1. We conjecture that Remark 4.2.10 holds for a general link diagram.

Some properties of alternating links hold in a more generalized class of links. For example, Theorem 4.1.1 by Cromwell holds for homogeneous links. We end with following questions:

1. Under what conditions are quantities in Definition 5.3.2 invariant under Reidemeister moves?

2. Does any of the quantities in Definition 5.3.2 remain invariant for homogeneous links?

REFERENCES

[1] D. Rolfsen, *Knots and links*, vol. 346. American Mathematical Soc., 2003.

[2] C. C. Adams, *The knot book*. American Mathematical Soc., 1994.

[3] P. R. Cromwell *et al.*, *Knots and links*. Cambridge university press, 2004.

[4] G. Burde and H. Zieschang, "Knots," in *Knots*, de Gruyter, 2008.

[5] D. B. West *et al.*, *Introduction to graph theory*, vol. 2. Prentice hall Upper Saddle River, 2001.

[6] M. Mastin, "Links and planar diagram codes," *Journal of Knot Theory and Its Ramifications*, vol. 24, no. 03, p. 1550016, 2015.

[7] R. Merris, *Graph theory*. John Wiley & Sons, 2011.

[8] H. Whitney, "2-isomorphic graphs," *American Journal of Mathematics*, vol. 55, no. 1, pp. 245–254, 1933.

[9] H. Seifert, "Über das geschlecht von knoten," *Mathematische Annalen*, vol. 110, no. 1, pp. 571–592, 1935.

[10] J. W. Alexander, "A lemma on systems of knotted curves," *Proceedings of the National Academy of Sciences of the United States of America*, vol. 9, no. 3, p. 93, 1923.

[11] S. Yamada, "The minimal number of seifert circles equals the braid index of a link," *Inventiones mathematicae*, vol. 89, no. 2, pp. 347–356, 1987.

[12] Y. Diao, G. Hetyei, and P. Liu, "The braid index of reduced alternating links," in *Mathematical Proceedings of the Cambridge Philosophical Society*, vol. 168, pp. 415–434, Cambridge University Press, 2020.

[13] Y. Diao, C. Ernst, G. Hetyei, and P. Liu, "A diagrammatic approach for determining the braid index of alternating links," *arXiv preprint arXiv:1901.09778*, 2019.

[14] K. Reidemeister, *Knotentheorie*, vol. 1. Springer-Verlag, 2013.

[15] V. F. Jones, "A polynomial invariant for knots via von neumann algebras," in *Fields Medallists' Lectures*, pp. 448–458, World Scientific, 1997.

[16] L. H. Kauffman, "State models and the jones polynomial," *Topology*, vol. 26, no. 3, pp. 395–407, 1987.

[17] W. W. Menasco and M. B. Thistlethwaite, "The tait flyping conjecture," *Bulletin (New Series) of the American Mathematical Society*, vol. 25, no. 2, pp. 403–412, 1991.

[18] W. Menasco and M. Thistlethwaite, "The classification of alternating links," *Annals of Mathematics*, vol. 138, no. 1, pp. 113–171, 1993.

[19] P. R. Cromwell, "Homogeneous links," *Journal of the London Mathematical Society*, vol. 2, no. 3, pp. 535–552, 1989.

[20] Y. Diao and V. Pham, "Writhe-like invariants of alternating links," *Journal of Knot Theory and Its Ramifications*, vol. 30, no. 01, p. 2150004, 2021.

[21] D. Bar-Natan, S. Morrison, *et al.*, "The mathematica package knottheory," *The Knot Atlas*.

[22] L. H. Kauffman and S. Lambropoulou, "On the classification of rational knots," *arXiv preprint math/0212011*, 2002.

[23] D.-Z. Du and K.-I. Ko, *Theory of computational complexity*, vol. 58. John Wiley & Sons, 2011.

[24] S. S. Skiena, *The algorithm design manual*, vol. 2. Springer, 1998.

[25] F. Jaeger, D. L. Vertigan, and D. J. Welsh, "On the computational complexity of the jones and tutte polynomials," in *Mathematical Proceedings of the Cambridge Philosophical Society*, vol. 108, pp. 35–53, Cambridge University Press, 1990.

[26] M. B. Thistlethwaite, "On the kauffman polynomial of an adequate link," *Inventiones mathematicae*, vol. 93, no. 2, pp. 285–296, 1988.

[27] J. C. Cha and C. Livingston, "Knotinfo: Table of knot invariants," 2011.

APPENDIX A: Some Computed Data

A.1 Prime Knot Diagrams Whose Simple Seifert Graphs are Hamiltonian

Below are the positions of alternating knots up to 14 crossings whose graphs $\tilde{G}_S(D)$ are Hamiltonian. For example, $5a_2$ is the first knot whose simple s-graph is Hamiltonian.

- 5-crossings: $\{2\}$.
- 7-crossings: $\{2, 3, 4, 5\}$.
- 9-crossings: $\{2, 3, 4, 5, 6, 7, 9, 10, 13, 16, 18, 23, 38\}$.
- 11-crossings: $\{94, 95, 123, 124, 186, 191, 192, 227, 234, 235, 236, 238, 240, 241, 242, 243, 244, 245, 246, 247, 263, 291, 292, 298, 299, 318, 319, 320, 329, 334, 335, 336, 337, 338, 339, 340, 341, 342, 343, 353, 354, 355, 356, 357, 358, 359, 360, 363, 364, 365\}$.
- 13-crossings:

  $\{809, 865, 866, 867, 868, 869, 1061, 1062, 1063, 1064, 1073, 1074, 1120, 1306, 1353, 1354, 1355, 1356, 1798, 1799, 1892, 1893, 1911, 1940, 1941, 1942, 1943, 2076, 2077, 2128, 2129, 2135, 2136, 2137, 2148, 2149, 2216, 2256, 2333, 2334, 2342, 2536, 2538, 2539, 2705, 2724, 2725, 2758, 2759, 2760, 2773, 2777, 2851, 2856, 2857, 2858, 2859, 2867, 2871, 2954, 2955, 2957, 2970, 2977, 2983, 3023, 3040, 3059, 3092, 3093, 3094, 3096, 3097, 3099, 3101, 3102, 3103, 3104, 3110, 3111, 3112, 3113, 3114, 3115, 3116, 3117, 3123, 3124, 3125, 3126, 3127, 3128, 3129, 3130, 3132, 3133, 3134, 3135, 3136, 3137, 3138, 3139, 3140, 3141, 3142, 3143, 3338, 3377, 3378, 3379, 3380, 3381, 3594, 3595, 3685, 3686, 3687, 3691, 3712, 3713, 3714, 3715, 3716, 3962, 3971, 4054, 4068, 4069, 4083, 4084, 4085, 4086, 4087, 4095, 4099, 4105, 4106, 4190, 4195, 4196, 4212, 4213, 4214, 4215, 4216, 4217, 4233, 4302, 4303, 4304, 4331, 4332, 4366, 4368, 4369, 4379, 4380, 4381, 4382, 4383, 4386, 4387, 4388, 4390, 4395, 4396, 4453, 4454, 4459, 4464, 4492, 4493, 4547, 4548, 4549, 4550, 4551, 4552, 4555, 4556, 4558, 4559, 4560, 4561, 4562, 4563, 4564, 4565, 4566, 4567, 4568, 4569, 4570, 4571, 4572, 4573, 4739, 4740, 4757, 4763, 4764, 4770, 4771, 4772, 4773, 4774, 4780, 4781, 4787,$

4788, 4789, 4790, 4799, 4800, 4801, 4802, 4805, 4812, 4821, 4822, 4823, 4824, 4825, 4826, 4827, 4828, 4829, 4830, 4831, 4832, 4833, 4834, 4835, 4836, 4849, 4850, 4851, 4852, 4853, 4854, 4855, 4856, 4858, 4859, 4860, 4861, 4862, 4863, 4864, 4866, 4867, 4868, 4872, 4874, 4875}.

A.2 Signed Seifert Graphs

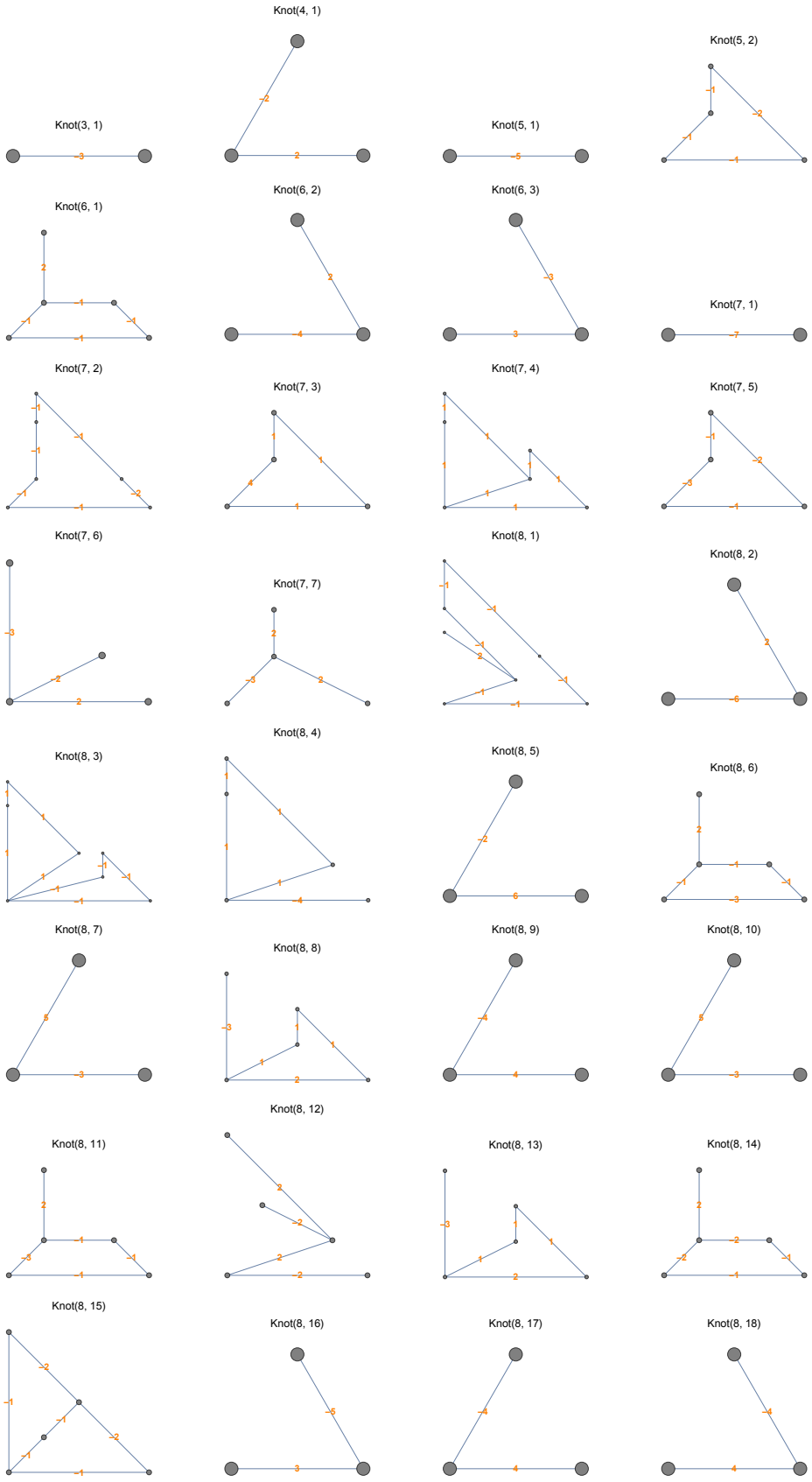

Figure A.1: Signed Seifert graphs of knot diagrams up to 8 crossings [1].

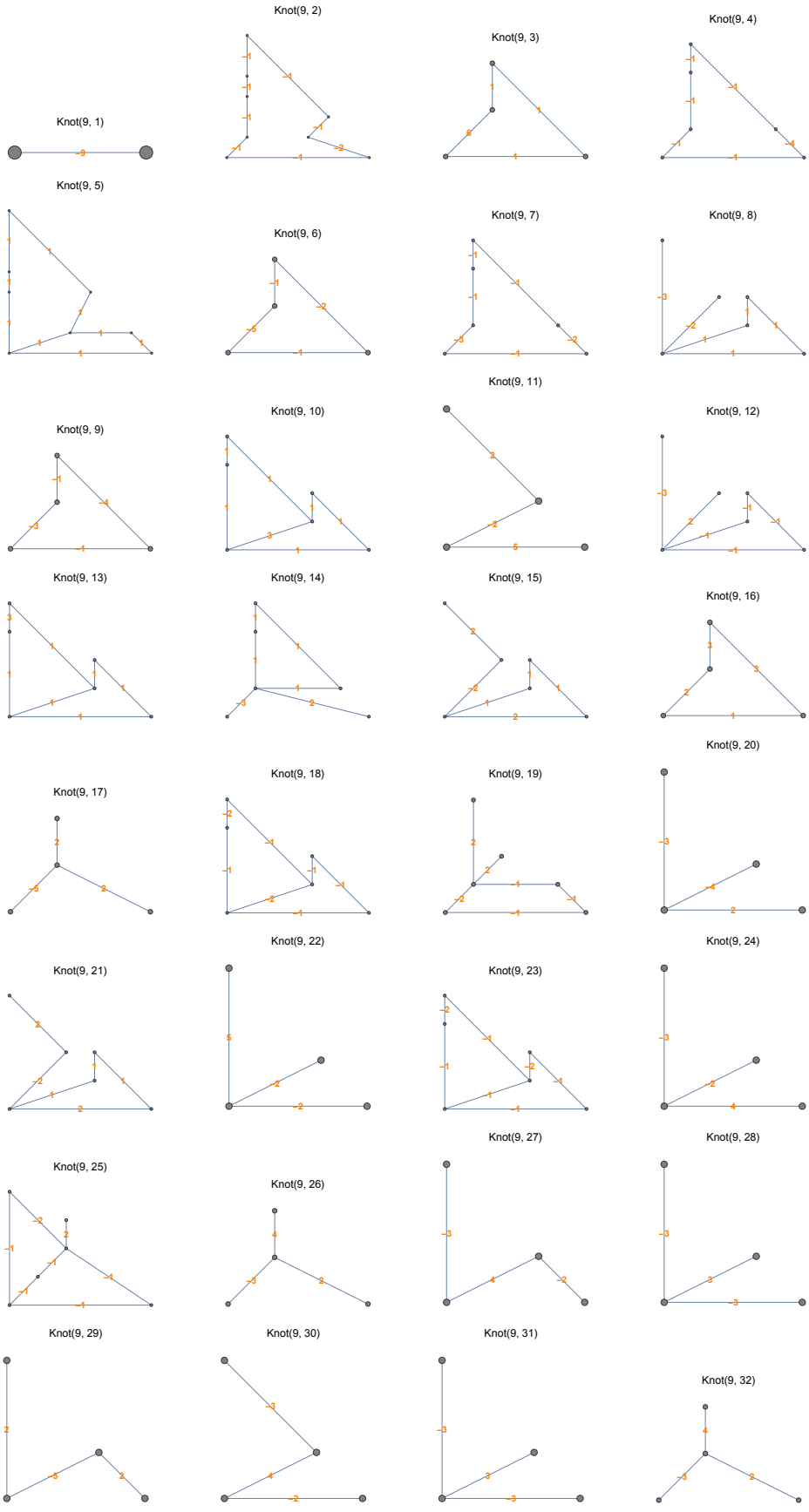

Figure A.2: Signed Seifert graphs of alternating knot diagrams of 9 crossings [1].

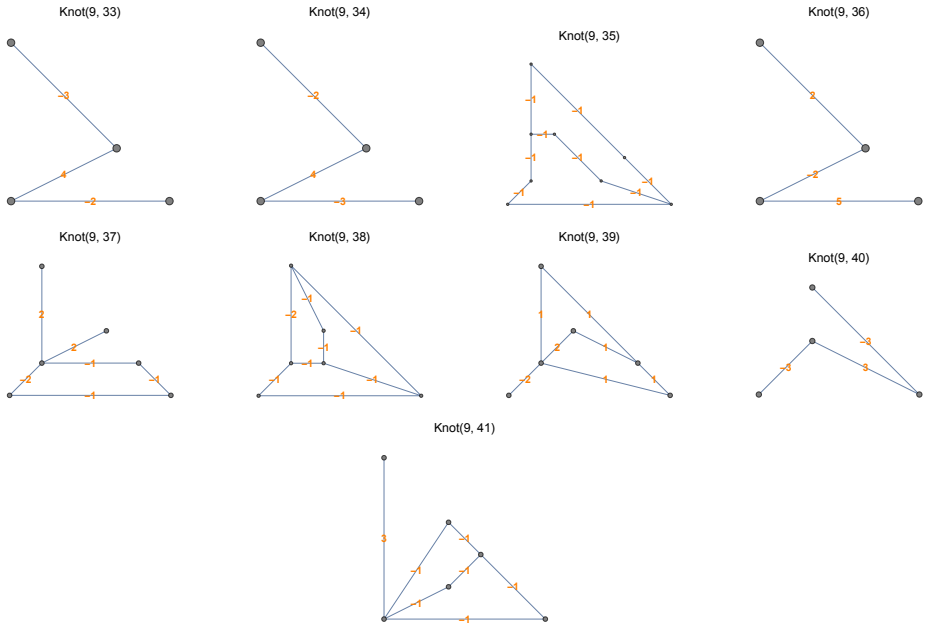

Figure A.3: (Continued) Signed Seifert graphs of alternating knot diagrams of 9 crossings [1].

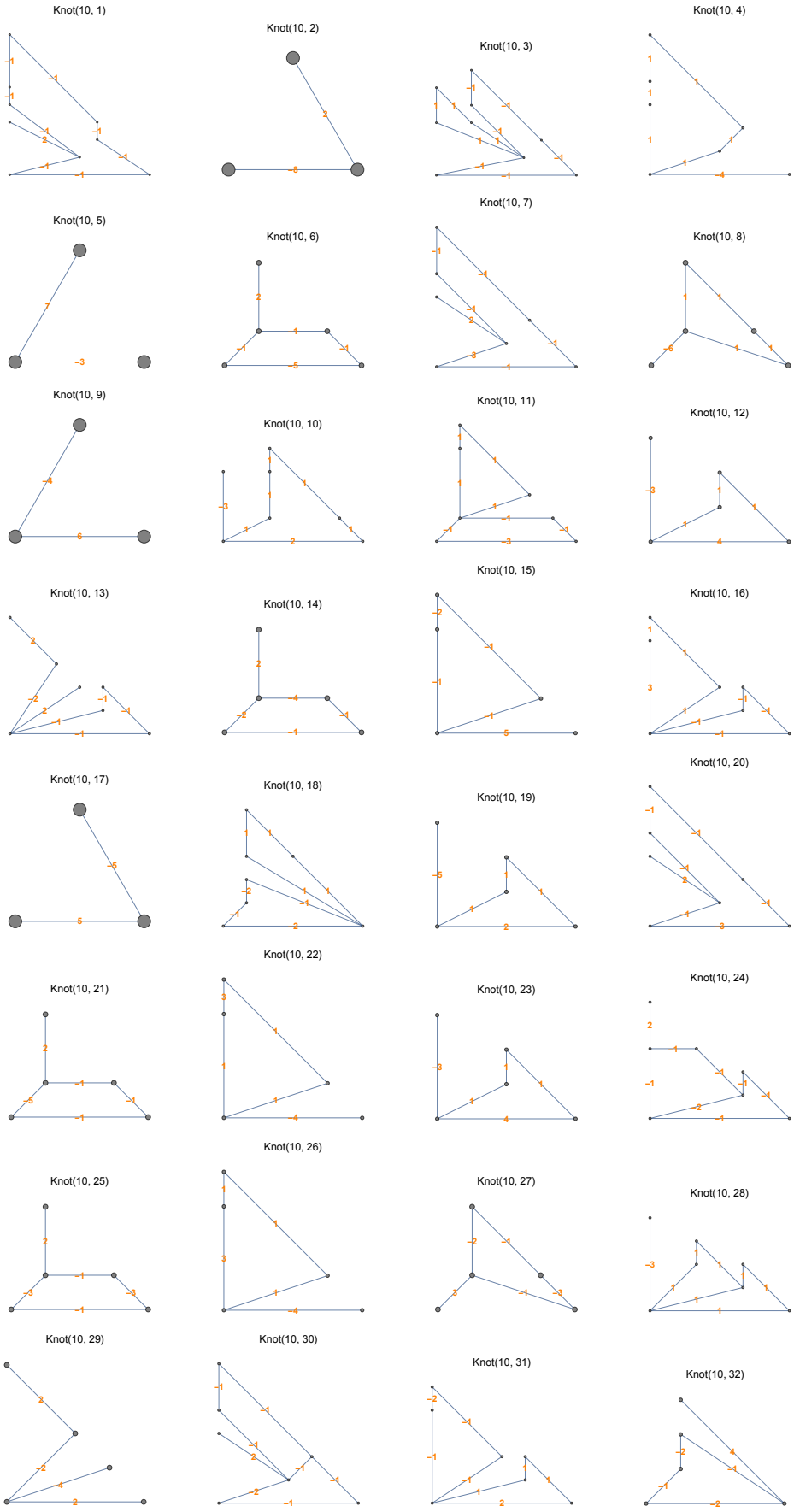

Figure A.4: Signed Seifert graphs of the first 32 alternating knot diagrams of 10 crossings [1].

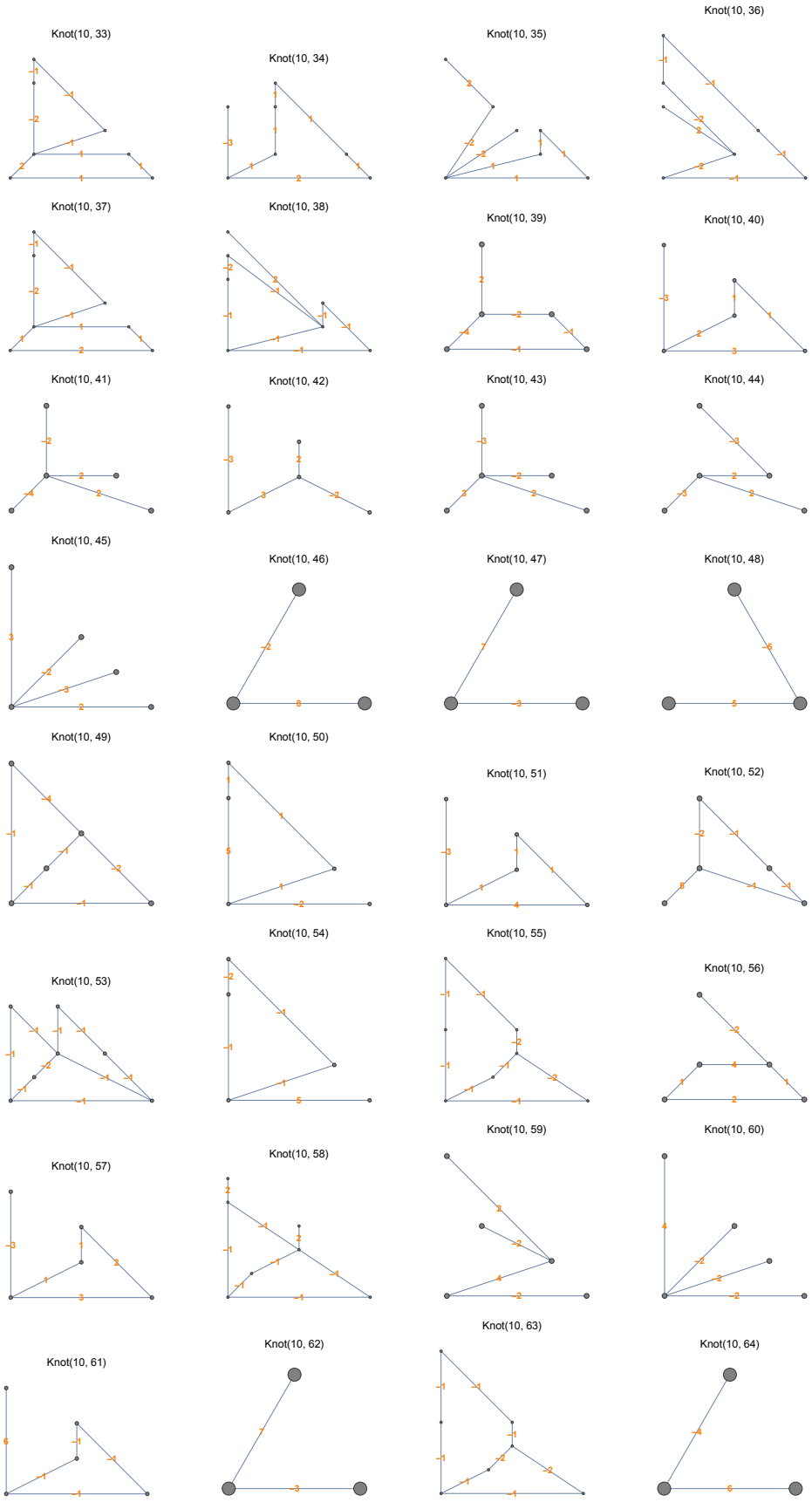

Figure A.5: (Continued) Signed Seifert graphs of alternating knot diagrams of 10 crossings [1].

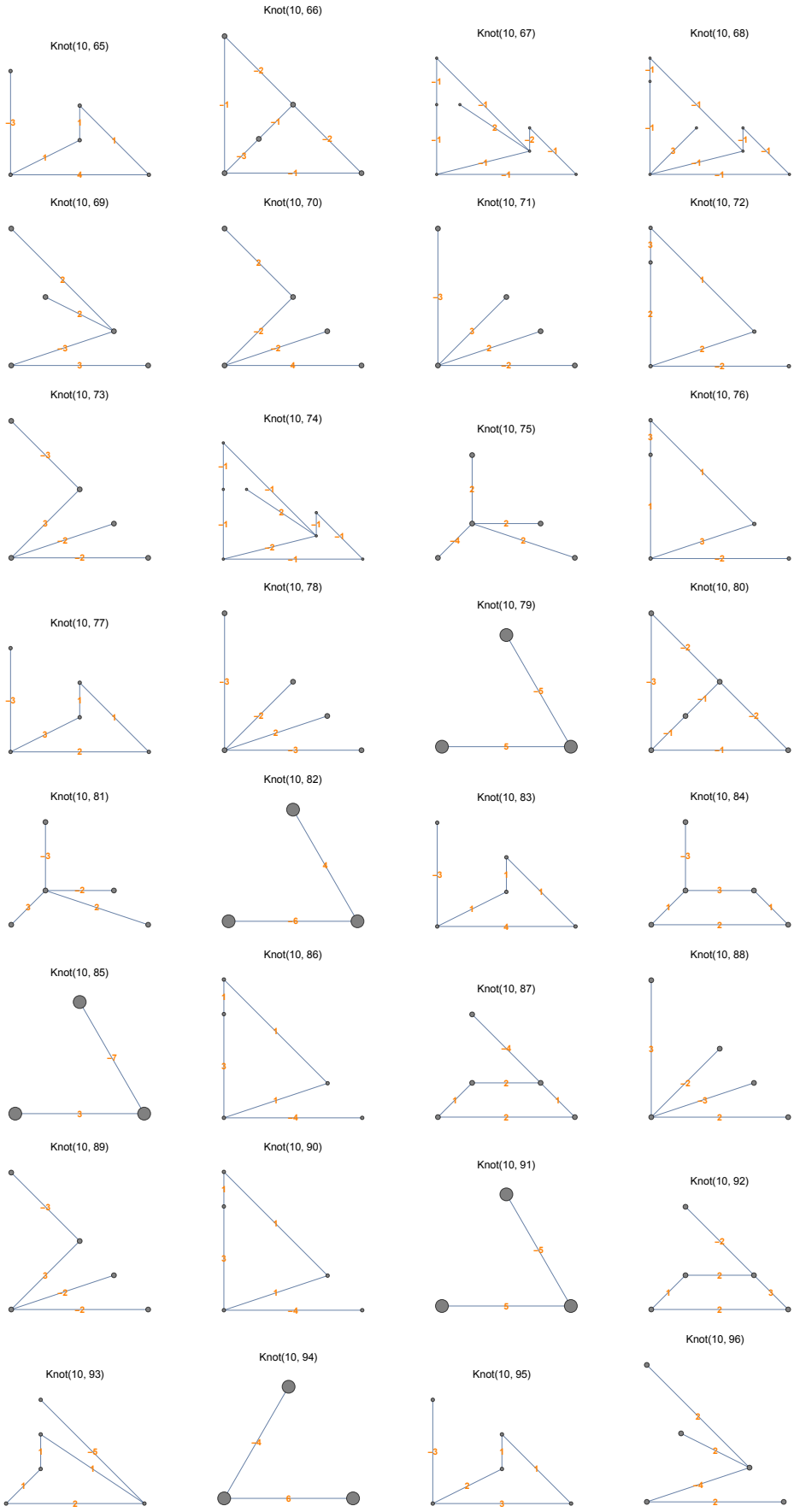

Figure A.6: (Continued) Signed Seifert graphs of alternating knot diagrams of 10 crossings [1].

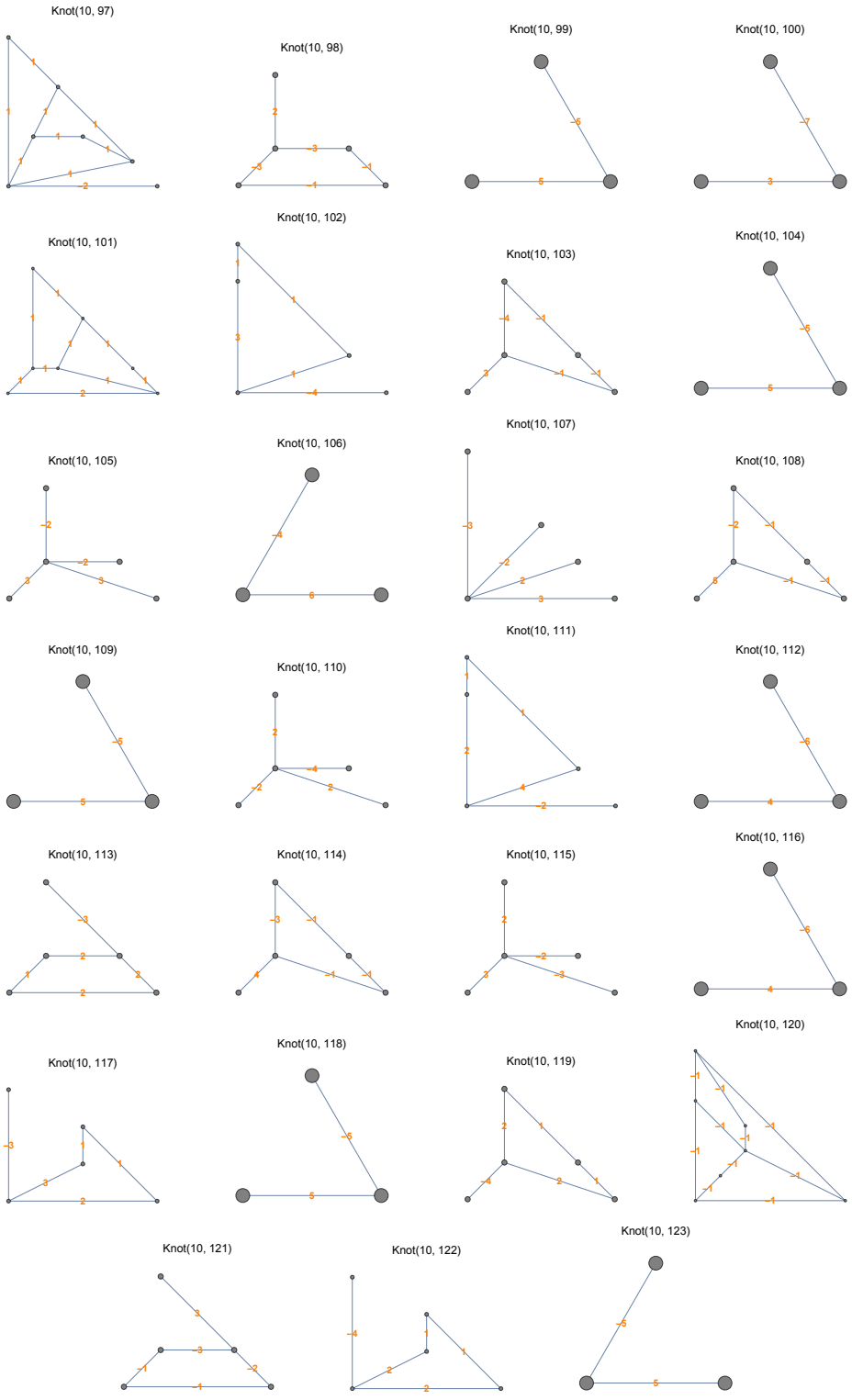

Figure A.7: (Last) Signed Seifert graphs of alternating knot diagrams of 10 crossings [1].

APPENDIX B: An Example of the Source Codes

```
DetectSCircles[knot_] :=
  Module[{
    cycles = List[],
    edge = -1,
    currentCycle = List[],
    foundCycle = False,
    tempEven = 0,
    filteredCrossings = List[],
    flattenedPd = List[],
    pd = PD[knot]},

   flattenedPd = Flatten[pd, 1, X];

   While[(Length[pd] * 2 > Length[Flatten[cycles]] ),
        For[i = 0, i < Length[flattenedPd], i++;
                If[MemberQ[Flatten[cycles], flattenedPd[[i]]] == False,

                                edge = flattenedPd[[i]];
                                Break[];]
        ]
     currentCycle = List[];
    AppendTo[currentCycle, edge];

    foundCycle = False;
```

```
  While[foundCycle == False,
   filteredCrossings =
    Select[Flatten[pd, 1, X], If[EvenQ[edge], EvenQ , OddQ]];
   For[j = -1, j < Length[filteredCrossings] - 2, j = j + 2;

    If[
     MemberQ[{filteredCrossings[[j]], filteredCrossings[[j + 1]]},
      edge],
              If[filteredCrossings[[j]] == edge,
              edge = filteredCrossings[[j + 1]],
              edge = filteredCrossings[[j]]]

              If[currentCycle[[1]] == edge,
              foundCycle = True;
              AppendTo[cycles, currentCycle];
              Break[];
              ]
               AppendTo[currentCycle, edge];]
    ] (*End inner For*)
   ]
  ] (*End big While*)
 Return[cycles, Module];
];
```